Modulation of *in vitro* osteoclastogenesis by glycated proteins

By

Mamun Or Rashid A N M

Thesis submitted for the degree of:

Doctor of Philosophy

In Medical Life Systems

Graduate school of Life and Medical Sciences

Doshisha University

Supervisor: **Prof. Yoshikazu Yonei**

Anti-Aging Medical Research Center and Glycation Stress Research Center

Graduate School of Life and Medical Sciences

Doshisha University

May 2017

Modulation of *in vitro* osteoclastogenesis by glycated proteins

Abstract

The differentiation and activation of osteoclast cells are of great importance in bone metabolism as osteoclasts resorb bone and activate osteoblast cells to rebuild the bone and thereby maintain bone quality and strength. Bone quality is an important factor that is determined by the native structure of the bone building blocks collagen (20% of bone weight), hydroxyapatite. Advanced glycation endproducts (AGEs) in human body (bone, serum, skin, urine etc.) increases with age and bone mineral density and bone quality decreases, resulting in high risk of big bone fracture. AGEs, such as N^{ε}-(carboxymethyl)-lysine (CML), pentosidine are elevated in serum of osteoporotic patients could be due to osteoclastic bone loss. Both osteoblast, osteoclast along with their precursors possess receptor for AGEs (RAGE) and it is a multifunctional receptor plays vital role in differentiation and inflammation. RAGE regulates osteoclastogenesis by binding with extracellular high mobility group box 1 (HMGB1) and activates osteoclastogenic downstream signals, thereby supports osteoclast cells to mature full functional. RAGE when binds with AGEs in regular culture media, it triggers to several cytokines such as, tumor necrosis factor alpha (TNFα), Interleukin 1 beta (IL-1β), Interleukin 6 (IL-6) production that are inflammatory and osteoclastogenic, too. Therefore, I investigated the effect of glycated proteins in RANKL-induced osteoclastogenesis in RAW264.7 cells.

The receptor activator of nuclear factor kappa-B ligand (RANKL) and Macrophage Colony-Stimulating Factor (M-CSF) are the main ligands known to induce osteoclastic differentiation (osteoclastogenesis) pathways and survival related pathways, respectively. In the present study, at first I examined whether both are require for *in vitro* osteoclastogenesis and survival of RAW264.7 cells. I found that RANKL alone at a concentration of 100 ng/mL could induce osteoclastogenesis by forming giant multinucleated osteoclast cells that also showed higher Tartrate-resistant acid phosphatase (TRAP) activity than in the presence of M-CSF. RANKL alone activated osteoclastogenic NF-κB, ERK, p-38 MAPK, NFATc1, and anti-apoptotic Akt in RAW264.7 cells and increased both maturation as well as activation markers such as Cathepsin-K (CTSK), V-type proton ATPase (Atp6v), TRAP, Matrix metallopeptidase 9 (MMP-9) mRNA expression. RANKL-induced osteoclastogenesis was not dependent on M-CSF, but was dependent on FBS, cell density, media content. This study shows that any change among essential components can lead to inappropriate *in vitro* osteoclastogenesis in RAW264.7 cells. Therefore, in rest of the experiments, I used 100 ng/mL RANKL in αMEM containing 10% FBS and cell density at 1×10^4 cells/well in 96-well plate and total 5 days of incubation.

Collagen is bone organic material that losses its native structure due to glycation stress. Collagen native structure is crucial for maintaining bone health. HSA is an abandoned protein in blood and thereby present in bone microenvironment. CML-HSA, pentosidine are most abundant AGEs found in osteoporotic patients. Therefore, I selected collagen type I, II, and HSA to investigate their effect on *in vitro* osteoclastogenesis. Glycated proteins were prepared using collagen-I or collagen-II or HSA incubating with glycating agents (glucose, fructose, glycolaldehyde, glyceraldehyde, glyoxal) in phosphate buffer (pH 7.4) and incubated at 60 °C for 24 or 40 h depending on the protein used. After glycation, non-reacted glycating agents and phosphate buffer were removed by ultrafiltration and used in *in vitro* osteoclastogenesis. Glycated proteins significantly modulated RANKL-induced osteoclastogenesis depending on the protein types and glycating agents; glucose and fructose derived glycated collagen-I and II significantly increased TRAP activity, whereas glycolaldehyde, glyceraldehyde, glyoxal derived glycated HSA and CML-HSA decreased. None of the experimental AGEs causes cell death in osteoclastogenic media. Glycation of collagen-I increased fluorescent AGE formation, fructose derived glycated collagen-I obtained 10 times higher fluorescent AGEs formation intensity, however, the effect was almost same as glucose derived glycated collagen-I that showed relatively lower fluorescence. In case of HSA, glycolaldehyde showed highest fluorescence intensity and highest inhibition of TRAP activity. CML-HSA also showed similar inhibitory effect demonstrated that the inhibition is due to AGEs. This data shows that glycated proteins significantly modulate RANKL-induced osteoclastogenesis.

As functional osteoclast are important for the removal of bone parts and the activation of bone forming osteoblast cells, and glycated-HSA inhibited osteoclastogenesis, demonstrated the formation of malfunctioning osteoclast by glycated-HSA and thereby alter bone remodeling. Therefore, I selected glycolaldehyde and glyceraldehyde derived glycated-HSA to investigate their mode of action. None of the glycated-HSA reduced early osteoclastogenic TRAF6, DC-STAMP, OC-STAMP, integrin β3 mRNA expression. Glycated-HSA inhibited RANKL-induced late osteoclastogenesis (3~5 days) as it reduced TRAP activity of 3 days RANKL-treated cells. However, RANKL+ HSA-AGEs treated cells rescued TRAP activity when the media was changed with RANKL alone after 3 days.

This data shows that HSA-AGEs can alter late osteoclastogenesis. Glycated-HSA did not induce TRAP activity in the absence of RANKL.

Secreted high mobility group box protein1 (HMGB1) is known to binds with receptor for AGEs (RAGE) and plays an important role on osteoclastogenesis. We found that glycolaldehyde and glyceraldehyde derived glycated-HSA inhibited RANKL-induced HMGB1 secretion,

downregulate osteoclastogenic nuclear factor-κB (NF-κB), nuclear factor of activated T-cells cytoplasmic 1 (NFATc1), c-Fos, calcium influx without altering RAGE expression.

Tables of Contents

Acknowledgements

Primarily, I would like to express my most heartfelt gratitude to Prof. Yoshikazu Yonei for accepting me as a PhD student in his laboratory, Anti-Aging Medical Research Center and Glycation Stress Research Center, Graduate school of Life and Medical Sciences, Doshisha University and enthusiastically teaching me. For all of the time, his expertise, his wide knowledge in various fields and his kindness have greatly helped me to increase my knowledge and to find the key to success in my research projects. The knowledge and supports that I have received from him are my motivation to fulfill my future career aspirations.

I am deeply thankful to Associate Prof. Wakako Takabe for guiding me systematically to accomplish the research projects and to increase my research skills. Without her tireless supervision, I would have never known how to conduct experiments well and understood different knowledge aspects at molecular levels.

I am also deeply grateful to Associate Prof. Masayuki Yagi who have given me special care, useful advices and supports during the time of my PhD study.

I am very grateful to all the professors of Graduate school of Life and Medical Sciences, Doshisha University who has provided me constructive suggestions to widen my work to a great improvement and supported me.

I would like to express my sincere gratitude to all members of Yonei Laboratory for helping me and sharing with me throughout my life in Japan.

I would like to take this special occasion to thank my parents, and brothers for their love and supports. My deep gratitude also goes to my dearest friends, teachers in and outside of Japan who have shared the precious moments during my PhD time.

Last, but not the least, I want to express my humble gratitude to the Lord of the Universe for helping me wherever I am!

---------Mamun Or Rashid A N M

List of abbreviations

Advanced glycation end products (AGEs)

ATPase H+ Transporting V0 Subunit D2 (Atp6v0d2)

Bovine serum albumin (BSA)

Cathepsin K (CTSK)

Cell counting kit-8 (CCK-8)

N^{ε}-(carboxymethyl)-lysine (CML)

Day (D)

Dendrocyte expressed seven transmembrane protein (DC-STAMP)

Dulbecco's modified Eagle's medium (DMEM)

Extracellular signal-regulated kinases (ERK)

Fetal bovine serum (FBS)

Fructose (Fru)

Glucose (Glu)

Glyceraldehyde 3-phosphate dehydrogenase (GAPDH)

Glycolaldehyde (Glycol)

Glyceraldehyde (Glycer)

Glyoxal (GO)

Hematopoietic stem cells (HSCs)

High mobility group box 1 (HMGB1)

Hour (h)

Human serum albumin (HSA)

Interleukin 1 beta (IL-1β)

Interleukin 6 (IL-6)

Inhibitor of the NFκB (IκBα)

Lactate dehydrogenase (LDH)

Macrophage colony-stimulating factor (M-CSF)

Matrix metallopeptidase 9 (MMP-9)

Messenger RNA (mRNA)

Mesenchymal stem cells (MSCs)

No transfection (NT)

Negative control (NC)

Nuclear factor kappa-B ligand (RANKL)

Nuclear factor-κB (NF-κB)

Nuclear factor of activated T-cells cytoplasmic 1 (NFATc1)

Osteoclast stimulatory transmembrane protein (OC-STAMP)

Potential of hydrogen (pH)

P38 mitogen-activated protein kinases (p38MAPK)

Radioimmunoprecipitation assay buffer (RIPA buffer)

Receptor for AGEs (RAGE)

Real-time polymerase chain reaction (RT-PCR)

Small interfering RNA (siRNA)

siHMGB1 (Si)

Sodium dodecyl sulfate polyacrylamide gel electrophoresis (SDS-PAGE)

Standard error of the mean (SEM)

Tartrate-resistant acid phosphatase (TRAP)

Tumor necrosis factor alpha (TNFα)

TNF receptor associated factor (TRAF)

1 Introduction

1.1 Bone remodeling

Bone remodeling (or bone homeostasis) is a lifelong process that serves to regulate bone structure to meet changing mechanical requirements and to repair micro damages or fractures in the bone matrix by maintaining plasma calcium homeostasis. Bone remodeling begins with the removal of mineralized bone through osteoclasts (a process called bone resorption) followed by the activation of bone forming osteoblast cells to recover the bone matrix that will subsequently become mineralized (ossification or new bone formation). Osteoclasts are originated from Hematopoietic stem cells (HSCs) and osteoblasts are from Mesenchymal stem cells (MSCs). Therefore, the differentiation of these two cell types plays crucial role in bone remodeling and thereby, maintaining bone strength [1,2]. The osteoclastic differentiation and activation are triggered mainly by osteoblast cells. After osteoclast cells resorb the bone parts, they activate osteoblast cells to rebuild the bone. The major biological regulators of bone remodeling include parathyroid hormone (PTH) and calcitriol as well as other hormones including growth hormones, glucocorticoids, thyroid hormones, sex hormones, insulin-like growth factors (IGFs), prostaglandins, bone morphogenetic proteins (BMP), tumor growth factor-beta (TGF-β), and cytokines e.g. M-CSF, RANKL, VEGF, IL-6 [1,3,4]. Any imbalance

between bone resorption and bone formation, can lead to many metabolic bone diseases, such as osteoporosis, rickets, osteomalacia (softening of the bones), osteogenesis imperfecta (a group of genetic disorders that mainly affect the bones that break easily), marble bone disease (osteopetrosis) and Paget's disease of the bone [5].

Osteoclast formation and functions are regulated by cytokines, primarily the receptor activator of NF-κB ligand (RANKL) and macrophage-colony-stimulating factor (M-CSF) via the activation of numerous signaling pathways, which are potential therapeutic targets to recover bone diseases. It is important to note that osteoclastic cells also regulate osteoblastic bone formation, both positively and negatively [6]. Aside from RANKL and M-CSF, there are several inflammatory cytokines, e.g. TNFα, IL-1 and IL-6, that are secreted by the macrophage under certain conditions which can also lead to osteoclastogenesis, leading to unnecessary bone resorption and thus causing inflammatory bone diseases like osteoarthritis and rheumatoid arthritis [5,7]. Therefore, not only osteoclastogenesis, but also its mediators are important as well.

M-CSF is reported to enhance mature osteoclast (OC) survival, motility and resorbing activity, possibly mediated by ERK upstream of the c-fos [8]. However, the role of M-CSF in the regulation of osteoclast differentiation remains unclear.

1.2 Glycation

Glycation is the non-enzymatic reaction between a sugar molecule, such as glucose or fructose, and a protein or lipid molecule [9] and thereby produce advanced glycation end products (AGEs) such as N^{ε}-carboxymethyl lysine (CML) [10], pentosidine [11], N^{ω}-carboxymethylarginine (CMA) [9] and alters the protein's native structure.

AGEs in human body (bone, serum, skin, urine etc.) increases with age and bone mineral density decreases, resulting in high risk of big bone fracture. Bone quality is also an important factor in case of determining bone strength. It is determined by the native structure of the bone building blocks collagen (20% of bone weight), hydroxyapatite. Collagen is organic material that losses its native structure due to reactive oxygen species, glycation stress and carbonyl stress, oxidative stress. Collagen native structure is crucial for maintaining bone health. CML-HSA, pentosidine are most abundant AGEs found in osteoporotic patients [12–16].

1.3 Glycation and bone remodeling

Both osteoblast, osteoclast along with their precursors possess receptor for AGEs (RAGE) and it is a multifunctional receptor plays vital role in differentiation. RAGE regulates osteoclastogenesis by binding with extracellular high mobility group box 1 (HMGB1) and activates osteoclastogenic downstream signals, thereby supports

osteoclast cells to mature full functional [17]. RAGE when binds with AGEs, it triggers to activate several cytokine such as, tumor necrosis factor alpha (TNFα), Interleukin 1 beta (IL-1β), Interleukin 6 (IL-6) production that are inflammatory and osteoclastogenic, too [7,18,19].

Pentosidine levels in bone collagen, serum and urine increase with age. The age-related AGE increase in bone and serum is a phenomenon observed in both men and women. The amount of AGEs formation and accumulation is positively correlated with age, whereas bone forming osteoblast cell differentiation correlates negatively [7,13,18,20,21]. Elevated level of AGEs in both male and female osteoporosis patients also demonstrated the link between AGEs and bone loss, and therefore fracture risk [14–16].

Bone is made of inorganic metal crystals, an organic extracellular matrix mainly type I collagen, lipids, water, bone forming cell osteoblast, osteocytes (trapped osteoblast in the osteoid), lining cell and bone resorbing cell osteoclast. Bone remodeling is a lifelong process of bone resorption and rebuild by the bone cells that are originated and differentiated from osteogenic stem cells [2,3,6]. Therefore, the differentiation, maturation, activation of these cells is of great importance in bone development. The amount of AGE formation and bone weakening are positively correlated with age and

both of the bone cells possess RAGE [17], therefore, there could be alteration in regulation of bone remodeling by the AGEs.

1.4 Objectives of the study

Previously one study in my lab found that CML-HSA can trigger the secretion of inflammatory and osteoclastogenic cytokine TNFα [19] in RAW264.7 cells in regular culture media. TNFα is inflammatory and osteoclastogenic too. AGEs can activate several pathways including NF-κB and thereby trigger TNFα production and the same pathway is used for osteoclastogenesis [7,18,20,22–24]. Therefore, I hypothesized that there could be effect of AGEs on osteoclastogenesis. To investigate the effect of AGEs on osteoclastogenesis, I used RAW264.7 cells. To prepare AGEs, I used collagen-I and II and human serum albumin (HSA) along with different glycating agents. The prepared AGEs were then used in osteoclastogenic cell culture medium to check their effect. At first, I set up a model system for *in vitro* osteoclastogenesis in RAW264.7 cells [4]. Then, I used this model for rest of the experiments. In this study, I checked the effect of different AGEs prepared using different proteins and glycating agents. Then I also checked their mode of action.

2 Materials and method

2.1 Cell culture and reagents

Murine monocyte/macrophage RAW264.7 (ATCC® TIB-71TM) cell line was purchased from American Type Culture Collection (ATCC; Manassas, VA). Cells were grown in Dulbecco's modified Eagle's medium (DMEM; Sigma-Aldrich, MO) supplemented with 10% fetal bovine serum (FBS) (Nichirei Biosciences, Tokyo, Japan), penicillin 100 units/mL, streptomycin 100 μg/mL and amphotericin B 25 μg/mL (Gibco, El Paso, TX) at 37 °C under the condition of 5% CO_2. Passage 3 to 6 were used for all experiments [4,19].

2.2 *In vitro* osteoclastogenesis

RAW264.7 cells were seeded in multi-well plates and incubated for 24 h. Then media were exchanged with αMEM (Gibco, El Paso, TX) or DMEM, with or without proteins as indicated in the figures with FBS, recombinant mouse RANK Ligand (rmRANKL) and M-CSF (R&D systems, MN) in the presence of antibiotics. After 3 days, the medium was renewed [19]. After 5 days of cultures, cells were observed by multiple assays as mentioned.

2.3 TRAP staining

Cells were fixed in a 10% formalin neutral buffer solution and stained using a TRAP staining kit (Cosmo bio co., LTD., Tokyo, Japan) according to the manufacturer's instruction. TRAP is a widely-used marker of osteoclast maturation and function. Multinucleated cells having ≥4 nuclei were counted under a light microscope as an osteoclast cell [19].

2.4 TRAP activity

Cells were fixed using a cell fixation buffer (Acetone: Ethanol=1:1) and then used to measure TRAP activity with a TRAP solution kit (Oriental Yeast Co., Tokyo, Japan) per the manufacturer's instruction. Colorimetric absorbance were taken at 405nm using a Varioscan® Flash (Thermo scientific, Waltham, MA) microplate reader [19].

2.5 Evaluation of cell viability

Cell viability was evaluated using cell counting kit-8 (Dojindo, Kumamoto, Japan). RAW264.7 cells were seeded on 96-well plates at the mentioned density and were treated as regular experiments described in the results section. After 5 days, a 10% volume of WST-8 solution was added to the culture medium and the cells were incubated for 1 h. Absorbance at 450 nm was then measured as previously described using a Varioscan® Flash microplate reader [19,25].

To check cytotoxic cell death, LDH assay was performed. RAW264.7 cells were seeded and treated as regular experiments done. Then, cultured media (50 μL) from each well was collected and used to determine the cell cytotoxicity (LDH secretion into media) in RAW264.7 cells. After incubating with assay solution and red color development, colorimetric absorbance was measured at 490 nm [26].

2.6 Glycated-protein preparation

To prepare glycated-collagen, we used 0.6 mg/mL collagen-I (bovine skin collagen type I (Nippi, Adachi-ku, Tokyo, Japan)) or collagen-II (bovine nasal septum EPC (Elastin products co. INC, MO)) along with 0.4 M glucose (Glu) or fructose (Fru) in 0.05 M phosphate buffer (pH 7.4) and incubated at 60 °C for 24 h. In case of heated-collagen, we used milliQ instead of glycating agents [27,28].

To prepare glycated-HSA, we used 8 mg/mL HSA along with several glycating agents, 0.2 M glucose (Glu) or fructose (Fru), or 33 mM glycolaldehyde (Glycol) or glyceraldehyde (Glycer) or Glyoxal (GO) in 0.05 M phosphate buffer (pH 7.4) and incubated at 60 °C for 40 h. In case of heated-HSA, we used milliQ instead of glycating agents [27]. After then, we removed remaining unreacted glycating agents and phosphate buffer using Amicon ultra-4 10K (Millipore, Darmstadt, Germany) centrifugal devices according to the manufacturer's instruction. Briefly, 4 mL of protein

mixture was placed into the centrifugal devices and centrifuged at 7,500 ×g for 15 min. Then washed using sterile milliQ and centrifuged again to collect heated or glycated proteins. Protein amount was measured using DC protein assay (Bio-Rad, Hercules, CA) for collagen and BCA protein assay (Thermo scientific, Rockford, IL) for HSA. CML-HSA was purchased from CircuLex (Nagoya, Aichi, Japan) [26,28].

2.7 Measurement of fluorescent AGEs in our experimental samples

Purified filtrated protein samples (AGEs or heated; 200 µg/mL for collagen-I and 150 µg/mL for HSA) were used to measure fluorescence intensity. Quinine sulfate solution was used as a reference for calibration of fluorescent materials and fluorescence intensity was measured at 370/440 nm using a Varioscan® Flash (Thermo scientific, Waltham, MA) microplate reader [26–29].

2.8 Isolation of total RNA and RT-PCR

RAW264.7 cells were seeded into 24-well plates at a density of 4×10^4 cells/well and incubated for 24 h. Then, media were changed and incubated as mentioned time and conditions. Then, total RNA was extracted using Isogen II reagent (Nippon Gene, Tokyo, Japan) according to the manufacturer's protocol. Five-hundred ng total RNA was reverse-transcribed with PrimeScriptTM RT Master Mix (Takara Bio Inc., Shiga, Japan) using Applied Biosystems 2720 Thermal cycler (Thermo Fisher Scientific, MA).

RT-PCR was performed with a Thunderbird™ SYBR qPCR mix (Toyobo Co., Osaka, Japan) per the manufacturer's protocol [4,26,28,30] with gene-specific primers (Invitrogen, Tokyo, Japan). The primers were used are as follows: NFATc1, 5′-GGA GCG GAG AAA CTT TGC G-3′ (forward), 5′-GTG ACA CTA GGG GAC ACA TAA CT-3′ (reverse); c-Fos, 5′-CGG GTT TCA ACG CCG ACT A-3′ (forward), 5′-TTG GCA CTA GAG ACG GAC AGA-3′ (reverse); Matrix metallopeptidase 9 (MMP-9), 5′-CTG GAC AGC CAG ACA CTA AAG-3′ (forward), 5′-CTC GCG GCA AGT CTT CAG AG-3′(reverse); Cathepsin K (CTSK), 5′-GAA GAA GAC TCA CCA GAA GCA G-3 (forward), 5′-TCC AGG TTA TGG GCA GAG ATT-3′ (reverse); Glyceraldehyde 3-phosphate dehydrogenase (GAPDH), 5′-AGG TCG GTG TGA ACG GAT TTG-3′ (forward), 5′-TGT AGA CCA TGT AGT TGA GGT CA-3′ (reverse) [31]; TRAP, 5′-GCG ACC ATT GTT AGC CAC ATA CG-3′ (forward), 5′-CGT TGA TGT CGC ACA GAG GGA T-3′ (reverse); ATPase H+ Transporting V0 Subunit D2 (Atp6v0d2), 5′-ACG GTG ATG TCA CAG CAG ACG T-3′ (forward), 5′-CCT CTG GAT AGA GCC TGC CGC A-3′ (reverse) [32]; TNFα, 5′- ACC CTC ACA CTC AGA TCA TCT TC-3′ (forward), 5′- TGG TGG TTT GCT ACG ACG T-3′ (reverse); IL-1β, 5′-TGT AAT GAA AGA CGG CAC ACC-3′ (forward), 5′-TCT TCT TTG GGT ATT GCT TGG-3′ (reverse); IL-6, 5′-ACA ACC ACG GCC TTC CCT ACT T-3′ (forward), 5′-CAC GAT

TTC CCA GAG AAC ATG TG-3′ (reverse); RAGE, 5′-ACT ACC GAG TCC GAG TCT ACC-3′ (forward), 5′- GTA GCT TCC CTC AGA CAC ACA-3′ (reverse) [26,28,30]; Traf6, 5′- GAA GAG GTC ATG GAC GCC AA -3′ (forward), 5′- CGG GTA GAG ACT TCA CAG CG-3′ (reverse); DC-STAMP, 5′- TCC TCC ATG AAC AAA CAG TTC CAA -3′ (forward), 5′-AGA CGT GGT TTA GGA ATG CAG CTC -3′ (reverse); OC-STAMP, 5′- ATG AGG ACC ATC AGG GCA GCC ACG -3′ (forward), 5′- GGA GAA GCT GGG TCA GTA GTT CGT-3′ (reverse) [33]; Integrin β3, 5′- TTA CCC CGT GGA CAT CTA CTA-3′ (forward), 5′-AGT CTT CCA TCC AGG GCA ATA-3′ (reverse) [17]; GAPDH was used as an internal control.

2.9 Protein Extraction and Western Blot Analysis

RAW264.7 cells were seeded in 6-well plate at a density of 2×10^5 cells/well and incubated for 24 h. They were then treated with αMEM supplemented with antibiotics and other proteins as mentioned in figures. The cells were then lysed with RIPA buffer containing 50 mM Tris-HCl, 150 mM NaCl, 0.1% SDS, 1% Triton ×-100 with complete protease inhibitor (Wako, Osaka, Japan) and phosphatase inhibitor (Roche Applied Science, Penzberg, Germany). Equal amounts of cell lysates (1~5 μg) were electrophoresed by SDS-PAGE (8~12% polyacrylamide), followed by the transferring of proteins on polyvinylidene difluoride (PVDF) membrane which were blocked with a

5% skim milk solution in TBS-T. Then membranes were immunoblotted with each primary antibody. The antibody against GAPDH, RAGE and HMGB1 was from Abcam (Cambridge, UK), while remaining antibodies were from cell signaling technology (CA). The antigen–antibody complexes were visualized with the appropriate secondary antibodies (Santa Cruz Biotechnology, CA) and chemiluminescence horseradish peroxidase (HRP) substrate along with detection system as recommended by the manufacturer [4,26]. The results illustrated in each figure are representative of three independent experiments. Image J was used to measure the optical density of protein bands.

2.10 siRNA experiments

For siRNA treatment we used lipofectamine RNAiMAX transfection reagent (Thermo Fisher Scientific) as manufacturer's protocol and allowed to grow for 3 days. To determine HMGB1 protein, which react by HMGB1 antibody and showed several bands, we used small interfering RNA against HMGB1 (siHMGB1 #s205520, Thermo Fisher Scientific, Waltham, MA) to transfect RAW264.7 cells. Then cell lysate and media were western blotted to check HMGB1 production and secretion. To check the effect of RAGE, we used siRAGE (#162189, Thermo Fisher Scientific) to transfect the cell. Then cells were treated as mentioned in the figures [26].

2.11 Nuclear and Cytoplasmic protein extraction

Nuclear and cytoplasmic extraction reagent kit (Thermo scientific, Rockford, IL, USA) was used to fractionate nuclear and cytoplasmic proteins as per manufacturer's protocol. Then protein lysate was used along with protease inhibitor, phosphorylase inhibitor to check protein expression or phosphorylation by western blot [26].

2.12 Measurement of intracellular calcium mobilization

Calcium mobilization from RANKL-treated RAW264.7 cells play important role in osteoclastogenesis. Therefore, we investigated the effect of glycated-HSA on RANKL-stimulated calcium mobilization using Fluo-8 no wash calcium assay kit (Abcam, Cambridge, UK) according to the manufacturer's protocol. Fluorescence intensity was measured at Excitation/emission (Ex/Em) = 490/525 nm using a Varioscan® Flash (Thermo scientific, Waltham, MA) microplate reader [26].

2.13 Statistical analysis

Data were expressed as mean ± the standard error of the mean (SEM). All statistical analyses were performed using the Tukey-Kramer test for intergroup comparison in each of the experiments. Results were considered significant at a significance level of 5%.

3 Results

3.1 Chapter 1: Establishment of an *in vitro* model for osteoclastogenesis

3.1.1 Effect of RANKL and M-CSF on multinucleated TRAP positive osteoclast cell formation:

RAW264.7 cells were treated with 0~100 ng/mL RANKL with and without 10 ng/mL M-CSF and then incubated for 5 days. After which, TRAP positive multinucleated osteoclast cells (≥4 nuclei and ≥10 nuclei) were counted under a light microscope. RANKL significantly increased multinucleated osteoclast (≥4 nuclei) cell formation up to 50 ng/mL RANKL, but the amount for 100 ng/mL did not differ from 50 ng/mL. However, giant multinucleated osteoclast (≥10 nuclei) formation was increased by RANKL dose dependently (Figure 1.1A-C). Osteoclastogenesis was unchanged in the presence of 10 ng/mL M-CSF with differing concentrations of RANKL (Figure 1.1B-C).

To further investigate on whether M-CSF has some effect on RANKL induced osteoclastogenesis, we used RANKL 100 ng/mL along with 0~50 ng/mL M-CSF. RANKL 100 ng/mL in the presence of M-CSF slightly increased small multinucleated osteoclast (≥4 nuclei) cell formation (Figure 1.1D-E), but significantly decreased large multinucleated osteoclast (≥10 nuclei) cell formation (Figure 1.1D, F) showing that M-CSF can either inhibit small osteoclast cell's fusion, or stimulate cell multiplication

rather than differentiate them. To confirm the effect of M-CSF on RANKL-induced osteoclastogenesis, we also checked TRAP enzymatic activity. TRAP activity was significantly increased dose dependently by RANKL (Figure 1.2A), while cell proliferation fell, suggesting a shift to differentiation (Figure 1.2B); M-CSF alone did not increase TRAP activity. RANKL 100 ng/mL along with M-CSF did not increase TRAP activity, moreover 50 ng/mL M-CSF decreased TRAP activity 20% compared to RANKL alone (Figure 1.2C) shows that RANKL can regulate osteoclastogenesis independent of M-CSF. Cell proliferation was not altered by M-CSF in the presence or absence of RANKL (Figure 1.2D), showing that RAW264.7 cells can grow and differentiate without M-CSF. RANKL treated cells compared to no-RANKL groups shows that cell multiplication falls due to differentiation by RANKL (Figure 1.2D).

3.1.2 FBS plays crucial role in RANKL-induced osteoclastogenesis: FBS is a widely used supplement for culture media, therefore, it is also important to know if there any effects of FBS on RANKL-induced osteoclastogenesis. To address this, RAW264.7 cells were treated with αMEM containing 0~10% FBS, with and without 100 ng/mL RANKL, for 5 days. TRAP activity was not significantly changed by FBS alone in the absence of RANKL (Figure 1.3A). RANKL 100 ng/mL failed to induce osteoclastogenic TRAP activity in the absence of FBS (Figure 1.3A). However, in the presence of 2.5 or 10%

FBS, osteoclastic TRAP activity was significantly induced showing that FBS plays a vital role in RANKL-induced osteoclastogenesis. Cell proliferation was also significantly increased by FBS regardless of RANKL concentration. Without FBS, cells grown showed almost 80% mitochondrial activity (WST-8 assay) (Figure 1.3B), but osteoclastogenesis could not be induced.

3.1.3 Effect of initial cell number on RANKL-induced osteoclastogenesis: RAW264.7 cells underwent multiplication first upon RANKL stimulation. The new cells then fused together and formed small-multinucleated transparent osteoclast cells on day 2 (Figure 1.4A). After this, the small osteoclast cells fused together and formed giant multinucleated (≥10 nuclei) transparent osteoclast cells (day 3, 4). On day 5, these giant osteoclast cells matured and lost their transparency, possibly due to alternate protein synthesis. Without RANKL, cells simply multiplied without fusing. As we found, RANKL treatment induced multiplication first, so the low cell number may be a possible cause. Therefore, we checked whether a higher initial cell number could induce osteoclastogenesis more or not next. Cells were seeded at 1×10^4 cells/well and 2×10^4 cells/well in 96-well plate. TRAP activity was significantly reduced by the greater cell number (Figure 1.4B) and cell proliferation was slightly increased (Figure 1.4C) showing that proper osteoclastogenesis requires a certain initial cell density and

RANKL-treated cells are programmed to multiply first, then new cells fuse together.

3.1.4 RANKL induced Osteoclastogenic mRNA expression independent of M-CSF: Since RANKL 100 ng/mL with 10% FBS containing αMEM significantly induced osteoclastogenic TRAP activity and multinucleated TRAP positive cell (≥10 nuclei) formation in the absence of M-CSF, we checked whether RANKL alone could induce other osteoclastogenic gene expression using RT-PCR. Cells were seeded in 24-well plates at a density of 4×10^4 cells/well and incubated for 24 h. The cells were then treated with αMEM supplemented with 10% FBS and antibiotics with and without 100 ng/mL RANKL. mRNA expression of the nuclear factor of activated T cells (NFATc1), the master transcription factor for osteoclast differentiation, was significantly induced by RANKL 100 ng/mL, peaking after 6h of treatment before declining (Figure 1.5A). Other osteoclast maturation and activation marker genes *i.e.* CTSK, Atp6v, TRAP, MMP-9 mRNA expression was also significantly induced by RANKL and peaked after 5 days of treatment (Figure 1.5B). This data shows that RANKL alone can induce proper osteoclastogenesis in the absence of M-CSF.

3.1.5 Effect of media content on RANKL induced osteoclastogenesis: RAW264.7 cells were treated with RANKL 100 ng/mL in αMEM or DMEM to check whether the medium itself has effect on osteoclastogenesis or not. TRAP activity was not changed

by media content (Figure 1.6A), but TRAP, MMP9, CTSK, Atp6v mRNA expression was significantly reduced in DMEM after 5 days of treatment (Figure 1.6C). Cell proliferation was significantly increased in DMEM compared to αMEM (Figure 1.6B). A possible cause being the downregulation of osteoclastogenic mRNA expression as we normalized the data using GAPDH. DMEM may induce cell proliferation along with differentiation in the presence of RANKL.

3.1.6 RANKL activated both osteoclastic and survival related pathways: To check the effect of RANKL on osteoclastogenic and survival related pathway activation, RAW264.7 cells were seeded in a 6-well plate at a density of 2×10^5 cells/well and incubated for 24 h. Followed by treatment with αMEM supplemented with 10% FBS, antibiotics and 100 ng/mL RANKL for up to 60 min. The cell lysates were then used for western blot against mentioned proteins. RANKL treatment activated phosphorylation of osteoclastogenic NF-κB, ERK, p38 MAPK and survival related Akt(Thr308) pathways, but not pAkt(Ser473) (Figure 1.7A-B) in the absence of M-CSF showing that RANKL itself can trigger both the survival and differentiation of RAW264.7 cells.

3.1.7 Schematic representation of RANKL-induced osteoclastogenesis in RAW264.7 cells: In our experiments, we used TRAP staining and activity, multinucleated cell numbers, cell morphology; NFATc1, CTSK, Atp6v, TRAP, MMP9

mRNA expression as osteoclastogenic markers. RANKL regulation of RAW264.7 cell osteoclastogenesis in our *in vitro* model was found to be independent of M-CSF; dependent on FBS, media content and cell density (Figure 1.8). Therefore, in rest of the experiments, αMEM containing 10% FBS, RANKL 100 ng/mL in the presence of antibiotics and cell density 1×10^5 cells/mL was used for optimum osteoclastogenesis.

3.2 Chapter 2: Effect of glycated proteins on RANKL-induced osteoclastogenesis

3.2.1 Glycated-collagen-I stimulated RANKL-induced osteoclastogenesis in RAW264.7 cells: RAW264.7 cells were treated with RANKL 100 ng/mL with or without glycated-collagen-I (Glucose or fructose derived glycated collagen-I; Col-I-Glu, Col-I-Fru, respectively) for 5 days and then osteoclastogenesis was evaluated by TRAP activity and cell cytotoxicity was evaluated using WST-8 assay and LDH secretion into media. Glycated-collagen-I showed no effect on RANKL-induced osteoclastogenesis in lower concentration (5~50 µg/mL, Figure 2.1A), but at higher concentration (200 µg/mL, Figure 2.1B) significantly stimulated without causing cell death (Figure 2.2A-B). As RAW264.7 cells also show TRAP activity when they are activated, therefore, I also checked the effect of glycated-collagen-I in the absence of RANKL and found to have no such stimulatory effect on TRAP activity in RAW264.7 cells (Figure 2.1B).

3.2.2 Fluorescent AGEs produced in glycation models: Glycation of proteins is reported to produce fluorescent AGEs, therefore we checked fluorescence intensity of the glycated-collagen-I at a concentration of 200 µg/mL as its effective dose. Col-I-Fru showed highest fluorescence intensity compared to Col-I-Glu and Col-I-Heated (Figure 2.3). Even though Col-I-Fru and Col-I-Glu showed similar effect on osteoclastogenesis,

but their fluorescence intensity was too different, indicating that the effect of glycated-collagen-I derived fluorescence AGE on TRAP activity may have less contribution.

3.2.3 Glycated Collagen-II stimulated RANKL-induced osteoclastogenesis in RAW264.7 cells: As we found glycated-collagen-I stimulated RANKL-induced osteoclastogenesis in RAW264.7 cells, we also checked the effect of glycated-collagen-II (Col-II-Glu, Col-II-Fru). Both Col-II-Fru and Col-II-Glu 200 µg/mL also stimulated RANKL-induced osteoclastogenesis (Figure 2.4A) without causing cell death (Figure 2.4B).

3.2.4 Glycated-HSA inhibited osteoclastic differentiation of RAW264.7 cells depending on glycating agents and fluorescence intensity: HSA is one of the main protein that is present in high amount in blood circulation and thereby present in bone microenvironment. Therefore, we investigated the effect of glycation of HSA on RANKL-induced osteoclastogenesis in RAW264.7 cells. We used native, heated, glycated (using glucose, fructose, glycolaldehyde, glyceraldehyde, glyoxal) HSA (500 µg/mL) in the presence of 100 ng/mL RANKL for 5 days. Then TRAP activity was measured. As shown in Figure 2.5A, native, heated and HSA-Glu, HSA-Fru have no effect on TRAP activity, whereas, HSA-Glycol, HSA-Glycer, HSA-GO significantly reduced TRAP activity without causing cell death (Figure 2.5B-C). Therefore, next we

checked cell morphology under microscope to investigate whether HSA-Glycol and HSA-Glycer inhibited the differentiation or activation of differentiated cells. We found that differentiation was inhibited without causing cell death (Figure 2.5D). As glycation produce fluorescence AGEs, so we checked the fluorescence intensity of 150 µg/mL glycated-HSA. Fluorescence intensity was significantly increased depending on the glycating agents, whereas, glucose-derived glycated-HSA (HSA-Glu) showed lowest and glycolaldehyde-derived glycated-HSA (HSA-Glycol) showed highest fluorescence intensity (Figure 2.5E), that also shows that glycolaldehyde reaction rate with HSA was highest among tested glycating agents.

3.2.5 Effect of glycated-collagen-I and glycated-HSA together on osteoclastogenesis: As we found glycated collagen-I to stimulate RANKL-induced osteoclastogenesis (Figure 2.1B) and in another study, we found glycolaldehyde and glyceraldehyde derived glycated-HSA (HSA-Glycol and HSA-Glycer, respectively) inhibited (Figure 2.5A, D) RANKL-induced osteoclastogenesis in RAW264.7 cells. Therefore, we also checked whether both of the stimulatory and inhibitory glycated proteins could neutralize each other's effect or not. Here we found HSA-Glycol and HSA-Glycer at a concentration of 150 µg/mL to inhibit and Col-I-Glu 200 µg/mL to stimulate as our previous study. However, when both were present together, TRAP

activity was significantly induced compared to glycated-HSA+RANKL treatment and decreased compared to Col-I-Glu+RANKL and RANKL alone group (Figure 2.6A). That shows glycation of proteins have either stimulatory or inhibitory effect depending on the protein type and together they can modulate RANKL-induced osteoclastogenesis without causing cell death in RAW264.7 cells (Figure 2.6B).

3.2.6 CML-HSA also inhibited RANKL-induced osteoclastogenesis: CML-HSA, a well-known AGE that is responsible for many pathological conditions and glycolaldehyde is known to produce CML-HSA. Therefore, we also checked the effect of CML-HSA (HSA and HSA-Heated as negative control) on RANKL-induced osteoclastogenesis. We found CML-HSA 0.5 µg/mL also significantly inhibited TRAP activity compared to RANKL with or without HSA and HSA-Heated (Figure 2.7A). CML-HSA increased cell number compare to RANKL treatment alone (Figure 2.7B).

3.2.7 Schematic representation of AGEs modulation of RANKL-induced osteoclastogenesis in RAW264.7 cells: Glycated collagen type I and II induced osteoclastogenic TRAP activity in our *in vitro* model. Whereas, glycated-HSA significantly inhibited. Both showed opposite effect on TRAP activity. When we used both Col-I-Glu and HSA-Glycol or HSA-Glycer together, TRAP activity were altered compared to all tested groups (Figure 2.8).

3.3 Chapter 3: Effect of glycated-HSA on RANKL-induced osteoclastogenesis

3.3.1 Glycated-HSA inhibited osteoclastogenic and inflammatory mRNA expression by RANKL-treated RAW264.7 cells: As glycated-HSA inhibited osteoclastogenesis, therefore, we investigated the effect of glycated-HSA on mRNA expression of osteoclastic maturation and activation marker genes (Figure 3.1A), early osteoclastogenic and fusion related marker genes (Figure 3.1B), and inflammatory and osteoclastogenic mRNA (TNFα, IL-1β, IL-6) expression (Figure 3.1C) by RAW264.7 cells in our experimental conditions. I found TRAP, CTSK, MMP9 mRNA expression were significantly inhibited, whereas, Atp6v, RAGE (Figure 3.1A) and TRAF-6, integrinβ3, DC-STAMP, OC-STAMP (Figure 3.1B) mRNA expression were remain unchanged in all tested time point except for the DC-STAMP which was induced by HSA-Glycol after 1 day. Glycated-HSA inhibited osteoclastogenic cytokine production. As glycated-HSA is also known for inducing osteoclastogenic and inflammatory cytokine production by macrophage cells, so next we checked whether HSA-Glycol and HSA-Glycer stimulate inflammatory mRNA expression in osteoclastogenic culture medium or not. We found that TNFα mRNA expression was fall down at 150 μg/mL, but significantly increased at higher concentration, 500 μg/mL, whereas, IL-1β, IL-6

mRNA expression was significantly fall down by glycated-HSA (Figure 3.1C). These data suggested that in osteoclastogenic media, glycated-HSA downregulate osteoclastogenesis and inflammatory effect but have no effect on early stage markers.

3.3.2 Effect of HSA-AGEs on osteoclastogenesis on early and later time point: Glycated-HSA showed no effect on early osteoclastogenic and fusion related markers like TRAF-6, Integrin β3, DC-STAMP, OC-STAMP after 1, 2 and 3 days (Figure 3.1B) of treatment. Therefore, we checked if there any effect of glycated-HSA on early or late osteoclastogenesis. We used to treat RAW264.7 cells with or without RANKL for 5 days as positive and negative control, respectively. Other conditions were,

- RANKL+HSA-AGEs treatment for 5 days for the inhibitory effect of HSA-AGEs,
- RANKL treatment for 0~3 days and then the media were changed with RANKL+HSA-AGEs for next 4~5 days to check the effect on late osteoclastogenesis,
- RANKL+HSA-AGEs treatment for 0~3 days and then the media were changed with RANKL for next 4~5 days to check the effect on early osteoclastogenesis,
- HSA-AGEs in the absence of RANKL.

In our experimental results (Figure 3.2A), we found HSA-AGEs to prevent late osteoclastogenesis as it reduced TRAP activity of 3 days RANKL-treated cells.

However, RANKL+ HSA-AGEs treated cells rescued TRAP activity when the media was changed with RANKL alone after 3 days that means removal of HSA-AGEs can overcome its effect on early osteoclastogenesis.

This data shows that HSA-AGEs can alter late osteoclastogenesis. Glycated-HSA did not induce TRAP activity in the absence of RANKL.

In addition, none of the experimental conditions induced cell death except for HSA-AGEs in the absence of RANKL and the αMEM (Figure 3.2B), which could be due to excess growth as in rest of the conditions RANKL shifted to differentiation and thereby reduced excess cellular growth.

3.3.3 HMGB1 expression and secretion in the experimental conditions: HMGB1 is a multifunctional nuclear protein that interacts with nucleosomes, transcription factors, and histones in the nucleus. However, when it is secreted, it binds with inflammatory receptor RAGE and plays vital role in cytokine production and in osteoclastogenesis. Therefore, we investigated the effect of glycated-HSA on HMGB1 expression and secretion and RAGE expression in the RAW264.7 cells. At first, we treated RAW264.7 cells with RANKL for different time points to check its effect on HMGB1 expression and secretion along with RAGE. In cell lysate, we found that HMGB1 expression was remain unchanged but RAGE expression was induced by RANKL treatment for 18 h to

3 days, and then declined (Figure 3.3A). HMGB1 secretion was observed after 36 h and reached at peak after 3 days of treatment, at day 4, it declined, as we had to replace the media after 3 days. As HMGB1 secretion was highest after 3 days, so we choose 3 days of incubation for rest of the experiments. HMGB1 antibody shows three different bands, so next we checked whether all are HMGB1 or not by using siHMGB1 transfection experiments and found siHMGB1 did not change HMGB1 production in cell, but secretion of all three bands were downregulated (Figure 3.3B).

Then we checked the effect of heated and glycated-HSA on HMGB1 expression and secretion and RAGE expression by RAW264.7 cells. HMGB1 and RAGE expression in cell lysate were not changed by glycated-HSA (Figure 3.4A), but HMGB1 secretion was fall down (Figure 3.4B). Next, we checked whether HMGB1 secretion inhibition is dose dependent or not. We checked 150 and 500 µg/mL of glycated-HSA, both of them reduced HMGB1 (25 kDa) secretion, but increased 17 kDa by HSA-Glycol (Figure 3.4C-D).

3.3.4 HMGB1 translocation from nucleus to cytoplasm also changed by glycated-HSA: As HMGB1 is a nuclear protein and it translocate into cytoplasm after RANKL stimulation, therefore, we investigated the effect of glycated-HSA on HMGB1 content in nucleus and cytoplasm after 3 days of RANKL treatment with or without glycated-

HSA. We found cytoplasmic HMGB1 (Figure 3.5A-B) and RAGE (Figure 3.5A, C) was not changed, but nuclear HMGB1 40 and 25 kDa amount was lower in HSA-Glycol treated cell (Figure 3.5A, D-E). Cytoplasmic proteins were normalized using GAPDH and nuclear protein using lamin A/C. HMGB1 is primarily located into nucleus (0 h), RANKL stimulation trigger translocation into cytoplasm. HSA-Glycol increased HMGB1 translocation from nucleus to cytoplasm, as nucleus is relatively too small compared to cytoplasm, so cytoplasmic HMGB1 was not changed with this additional nuclear HMGB1.

3.3.5 Effect of glycated-HSA on activation of osteoclastogenic pathways: As HSA-Glycol and HSA-Glycer significantly inhibited osteoclastogenesis; therefore, we investigated their effect on osteoclastogenic pathway activation. In cytoplasm, IκBα is degraded upon RANKL stimulation to activate NFκB and activated NFκB then translocate into nucleus. Therefore, we checked the effect of glycated-HSA on cytoplasmic IκBα degradation and nuclear NFκB (p65) activation. IκBα was degraded and was lowest in amount after 20 min of RANKL stimulation, but in the presence of glycated-HSA IκBα remain almost same amount (Figure 3.6A). NFκB (p65) translocation into nucleus also downregulated by glycated-HSA. This data suggested that glycated-HSA downregulated RANKL-induced NFκB (p65) activation (Figure

3.6A).

We also investigated the activation of p38MAPK and pERK in whole cell lysate. Phosphorylation of p38MAPK was not significantly changed, but pERK phosphorylation was significantly induced after 30~60 min of treatment with glycated-HSA (Figure 3.6B).

3.3.6 Effect of glycated-HSA on siRAGE treated RAW264.7 cell pathway activation: As glycated-HSA inhibited NFκB activation and induced ERK activation, therefore, we investigated whether this is done through RAGE or not. To check this, we transfected RAW264.7 cells using siRAGE to downregulate RAGE expression (Figure 3.7A). siRAGE significantly downregulated RAGE expression compared to both no transfection and negative control. Then siRAGE was used to transfect the RAW264.7 cells, and then, cells were treated with RANKL with or without glycated-HSA for 30 min. Whole cell lysate was prepared and used for western blot analyses to detect pERK, IκBα, p-p65, p65, GAPDH protein expression. Compared to Figure 3.6, in siRAGE treated cells, pERK was significantly downregulated in the presence of glycated-HSA and IκBα, p-p65 was not altered by glycated-HSA (Figure 3.7B), showing that RAGE plays crucial role on excess ERK activation and the inhibition of IκBα degradation by glycated-HSA.

3.3.7 Glycated-HSA and NFκB inhibitor inhibited osteoclastogenic NFATc1, c-Fos

mRNA expression: NFATc1 is the master transcription factor for osteoclastogenesis. c-Fos is also involved in osteoclastogenesis. Therefore, we also investigated whether glycated-HSA have any effect on NFATc1 and c-Fos expression or not. In our previous experiments, we found that NFATc1 expression was highest after 6 h of RANKL treatment [4]. Therefore, we checked the effect of glycated-HSA and NFκB inhibitor on NFATc1 and c-Fos expression after 6 h of treatment along with RANKL. NFκB inhibitor (BAY11-7082, 10μM) inhibited both NFATc1 and c-Fos in RANKL treated cells. In addition, HSA-Glycol and HSA-Glycer significantly inhibited NFATc1 and c-Fos mRNA expression at the dose of 150 and 500 μg/mL (Figure 3.8).

3.3.8 Effect of glycated-HSA on calcium influx activation: RANKL stimulation also activate calcium influx in macrophage cell to further activate osteoclastogenic pathways. We also investigated whether glycated-HSA inhibited calcium influx or not. We checked using Fluo-8 AM kit for up to 500 sec and found RANKL-stimulation significantly activated calcium influx, heated-HSA along with RANKL also activated immediately, but glycated-HSA inhibited calcium influx in our experimental conditions and the maximum intensity were also significantly low (Figure 3.9).

3.3.9 Schematic representation of mechanism of inhibition of RANKL signaling by HSA-AGEs: HSA-AGEs suppressed RANKL-induced activation of calcium influx, NFκB, c-Fos, NFATc1 seems to act via RAGE and the secretion of HMGB1 (Figure 3.10). Macrophage cell also possess scavenger receptor class A I and II, scavenger receptor class B CD36 and SR-B1 that are known for uptake and removal of foreign matters such as modified low-density lipoprotein, AGEs. Therefore, these receptors may play crucial role in response to different types of AGEs as HSA-Glu and HSA-Fru showed no effect.

.

4 Discussion

CML-HSA and pentosidine level was reported to be elevated in serum of osteoporosis patients [13–15]. Therefore, we investigated whether glycated protein can modulate osteoclastogenesis or not. We hypothesized either 1) glycated protein is stimulating osteoclastogenesis and thereby increasing bone loss or 2) inhibiting osteoclastogenesis and thereby inhibiting bone remodeling as functional osteoclast cells secrete required cytokines for osteoblastogenesis and therefore bone formation [3,6].

At first, I established an *in vitro* model for osteoclastogenesis in our lab. In the previous report, osteoclasts were completely absent in CSF-1 mutant mice with osteopetrosis, demonstrating the critical role of the macrophage-colony stimulating factor (M-CSF) in osteoclast differentiation from hematopoietic precursors [8,34–36]. Osteoclasts are differentiated cells of monocyte/macrophage lineage, originating from hematopoietic precursors. Thus, mutation in the CSF-1 gene may either block the differentiation of monocyte/macrophage from hematopoietic stem cells or directly block the osteoclastogenic differentiation of monocyte/macrophage. In this present study, I found that RAW264.7 cells osteoclastogenesis is regulated solely by RANKL alone. RANKL alone increased osteoclastogenesis in a dose dependent manner and showed best at 100 ng/mL (Figure 1.1A-C; and Figure 1.2A). M-CSF (50 ng/mL) in the presence of 100

ng/mL RANKL significantly increased small osteoclast (≥4 nuclei) formation (Figure 1.1D-E), but decreased giant multinucleated osteoclast (≥10 nuclei) formation (Figure 1.1D, F) and overall TRAP activity falls by 20% (Figure 1.2C). This shows that RANKL-induced osteoclastogenesis and osteoclast activation are not dependent on M-CSF in RAW264.7 cells. RANKL functions as a key factor for osteoclast differentiation, M-CSF did not induce osteoclastogenesis in either the absence or presence of RANKL. The reason for this could be either that M-CSF inhibits small osteoclast cell's fusion or that it stimulates cell proliferation rather than differentiation. However, M-CSF plays an important role in resorption by mature human osteoclast. M-CSF 10~25 ng/mL effectively augments RANKL-induced resorption, not by enhancing survival, but instead due to an increased activation of resorption in osteoclasts by potentiating RANKL-induced c-fos activation and extracellular signal-regulated kinase (ERK) 1/2 phosphorylation in mature OCs [8].

As RAW264.7 cells *in vitro* culture requires FBS, we checked whether FBS has any effect on osteoclastogenesis or not. FBS alone (10%) induces TRAP activity twice as much than with no FBS. RANKL 100 ng/mL was unsuccessful in inducing osteoclastogenesis in the absence of FBS (Figure 1.3A). FBS 2.5~10% significantly increased TRAP activity as well as cell proliferation, showing that FBS is essential for

both RAW264.7 cell proliferation and differentiation (Figure 1.3A-B). In a study by Wang *et al.,* it was presented that FBS promoted osteoclastogenesis in suitable concentrations by regulating the migration of osteoclast precursors and expressions of TRAP and CTSK [37]. FBS contains most of the factors required for cell attachment, growth, proliferation and differentiation and is thus used as an almost universal cell culture supplement for most types of human and animal cells. Although FBS has been in use for over 50 years, it remains uncharacterized. Recent proteomic and metabolomic studies revealed approx. 1,800 proteins and more than 4,000 metabolites present in the serum [38]. As RANKL cannot induce osteoclastogenesis in the absence of FBS, it shows that RANKL-induced osteoclastogenesis is very dependent on FBS. However, it is unclear which component(s) are playing a key role due to its very complex nature. As FBS is required for *in vitro* experiments, the possibility for false positive results in cases of RANKL inhibition studies is present if the samples inhibit the responsible component(s) of FBS; osteoclastogenesis be reduced without inhibiting RANKL-induced pathways.

RANKL treatment induced RAW264.7 cells to multiply first and new cells then fused together and formed giant osteoclast cells (Figure 1.4A). We used a high cell number (double) to check whether RANKL-treated cells can fuse together and increase TRAP activity or not. An increased cell number did not increase osteoclastogenesis

(Figure 1.4B), showing that fusion is happening between RANKL-induced new daughter cells which are proliferated to differentiate, not by the fusion between RANKL-induced parental cells. This data suggest that osteoclastic fusion requires new daughter cells originated from a RANKL-induced parental cell and that they are already programmed to fuse.

The nuclear factor of activated T cells (NFATc1) is known as the master transcription factor for osteoclast differentiation [22,39,40]. This factor was induced by RANKL 100 ng/mL in the absence of M-CSF and reached at peak after 6 h of treatment before declining in RAW264.7 cells (Figure 1.5A). Other osteoclast maturation and activation marker gene, *i.e.* CTSK, Atp6v, TRAP, and MMP-9 mRNA expression was also significantly induced by RANKL 100 ng/mL and reached their peaks after 5 days of treatment (Figure 1.5B). This data shows that RANKL alone can induce proper osteoclastogenesis by inducing osteoclastic gene expression in the absence of M-CSF [4].

Next, we considered the difference in the culture medium content. DMEM contains approximately four times as much of the vitamins and amino acids compared to the αMEM and two to four times as much glucose [41]. Osteoclastogenesis is coupled by several other cells such as MSC, osteoblast, osteocytes etc. Therefore, the co-culture of

the macrophage with them is also important in bone research, and many times, it requires DMEM. RAW264.7 cells were treated with RANKL 100 ng/mL in αMEM and DMEM to check whether DMEM can support osteoclastogenesis or not. TRAP activity was not changed (Figure 1.6A), but TRAP, MMP9, CTSK and Atp6v mRNA expression was significantly reduced in DMEM after 5 days of treatment (Figure 1.6C). Cell proliferation was increased in DMEM regardless of RANKL concentration, but decreased in αMEM with RANKL due to differentiation (Figure 1.6B). TRAP activity was induced in DMEM, but mRNA expression was reduced (Figure 1.6A, C). One possible reason could be that DMEM supports both proliferation and differentiation. Seeing, as we need to use a housekeeping gene to normalize any data, a high number of cell proliferation may lower the comparative mRNA expression in our results.

Osteoblast lineage regulates osteoclast differentiation and survival by synthesizing M-CSF and RANKL upon certain physiological conditions. Osteoclast differentiation *in vitro* depends on exogenous M-CSF [42], and M-CSF removal from purified osteoclast cultures from bone marrow results in apoptosis by activating caspase and MST1 kinase [43]. In another report, M-CSF was found to activate phosphoinositide 3-kinase (PI3K) and anti-apoptotic Akt kinase in osteoclast cells [44]. Akt activity is essential for cell survival. Akt target the apoptotic machinery like BAD, caspase-9, glycogen-synthase

kinase etc. [42,45,46]. RANKL and TNFα act primarily via NF-κB activation leading to the transcription and de novo synthesis of anti-apoptotic proteins [47]. However, some studies suggest that M-CSF, RANKL and TNFα, three cytokines with different functions, can stimulate the Akt pathway [5,20,24,48]. In our study, we found that RAW264.7 cells treated with 100 ng/mL RANKL without M-CSF in αMEM supplemented with 10% FBS and antibiotics activated osteoclastogenic NF-κB, ERK, p38 MAPK, along with anti-apoptotic Akt(Thr308) (Figure 1.7A-B) within 60 min of treatment, showing that the RANKL activation of these osteoclastic and survival pathways are independent of M-CSF.

RANKL-induced osteoclastogenesis was not dependent on M-CSF, but was instead dependent on FBS, cell density, media content (Figure 1.8). This study shows that any change among essential components can lead to inappropriate *in vitro* osteoclastogenesis in RAW264.7 cells. Therefore, in rest of the experiments, αMEM containing 10% FBS, RANKL 100 ng/mL in the presence of antibiotics and cell density 1×10^5 cells/mL was used for optimum osteoclastogenesis.

Next, I prepared AGEs as described in materials and method section and used in this *in vitro* osteoclastogenesis model of RAW264.7 cells. Our study indicated that glycated proteins affected RANKL-induced osteoclastogenesis both positively and negatively depending on the protein types used. Glycated collagen-I (the major organic component

of bone matrix) and collagen-II (the major organic component of cartilage) significantly increased RANKL-induced osteoclastogenesis at a dose of 200 µg/mL (Figure 2.1B and 2.4A), whereas, glycolaldehyde, glyceraldehyde and glyoxal derived glycated-HSA and CML-HSA significantly inhibited (Figure 2.5A and 2.7A) without causing cell death (Figure 2.2, 2.4B, 2.5B-C and 2.7B). Glycated collagen-I (Col-I-Glu) and HSA (HSA-Glycol or HSA-Glycer) together lessened RANKL-induced osteoclastogenesis compared to RANKL with or without Col-I-Glu groups and increased than glycated-HSA with RANKL groups (Figure 2.6A), shows that glycated proteins significantly alter the differentiation of RAW264.7 cells into osteoclast. CML-HSA, a major AGE, very common in osteoporotic patients [13–15], also showed inhibitory effect (Figure 2.7A) on osteoclastogenesis demonstrating the effect is due to AGEs.

Valcourt *et al* reported that AGE-modified (pentosidine) bone and ivory slices to inhibit resorption by mature rabbit osteoclast cells likely due to decreased solubility of collagen molecules in the presence of AGEs. Whereas, AGE-modified bovine serum albumin (BSA) totally inhibited murine and RAW264.7 cells osteoclast differentiation *in vitro* by impairing the commitment of osteoclast ancestors into pre-osteoclast cells [49]. Here, I investigated the effect of glycated collagen-I and II (in soluble form) and HSA on osteoclastogenesis in RAW264.7 cells. Bone resorptions usually occur when bone

microenvironment is altered. In our present study, we found glycation of soluble collagen-I and collagen-II significantly increased RANKL-induced osteoclastogenesis (Figure 2.1B and 2.4A), that shows glycation of collagen (bone protein) can stimulate osteoclastogenesis [28], that supports our first hypothesis.

Glycated protein amount in serum increased in osteoporotic patients [13,14]. In human body, HSA is present in blood and thereby in bone microenvironment, so we also checked if there is any effect of glycated-HSA on osteoclastogenesis. We observed that HSA-glycol and HSA-glycer affect negatively (Figure 2.5A, D) by downregulating RANKL-signalling [26] that supports our second hypothesis. That means, it also can interfere in osteoclastogenesis. Therefore, next we checked the effect of glycated collagen-I (glucose derived) and HSA-glycol or HSA-glycer together to check if they can counteract each other's effect. Both of the glycated proteins significantly counter each other's effect in our study (Figure 2.6A), provides evidence for modulation of osteoclastogenesis by glycated proteins.

CML-HSA is reported to produce by glycolaldehyde [50], therefore, we checked if CML-HSA have such effect on osteoclastogenesis. CML-HSA also significantly inhibited RANKL-induced osteoclastogenesis (Figure 2.7A), showing that glycated protein (AGEs) can alter osteoclastogenesis.

Glycation of protein was previously reported to produce fluorescence AGEs [4,27], therefore, we investigated fluorescence AGE formation by our experimental glycating agents. Fluorescence intensity of the glycated-collagen-I was measured at a concentration of 200 µg/mL as its effective dose. Col-I-Fru showed highest fluorescence intensity compared to Col-I-Glu and Col-I-Heated (Figure 2.3). Even though Col-I-Fru and Col-I-Glu showed similar effect on osteoclastogenesis, but their fluorescence intensity was too different, indicating that the effect of glycated-collagen-I derived fluorescence AGE on TRAP activity may less contribution. In case of glycated-HSA, lowest florescence intensity was shown by HSA-Glu, and highest by HSA-Glycol (Figure 2.5E). The possible reason could be the reaction rate as glucose, fructose are relatively too slow compared to rest of the glycating agents.

AGE-modified BSA was reported to totally inhibit *in vitro* osteoclastogenesis by impairing the commitment of osteoclast progenitors into pre-osteoclast cells through their interaction with specific cell-surface receptors as pre-osteoclast and osteoclast cells expressed several receptors including RAGE [49]. In our study, glycolaldehyde, glyceraldehyde, glyoxal-derived glycated-HSA significantly inhibited osteoclastogenic TRAP activity compared to RANKL alone, whereas, heated and glucose, fructose derived glycated-HSA showed no effect (Figure 2.5A) without causing cell death (Figure 2.5B-

C) that shows the inhibitory effect is glycating agent dependent. To check whether glycated-HSA inhibited osteoclastogenesis or the activation of osteoclast cells, we checked the cell morphology under microscope and found that glycated-HSA inhibited multinucleated osteoclast cell formation (Figure 2.5D) that is osteoclast differentiation is inhibited. In addition, all of the glycating agents that showed inhibitory effect on osteoclastogenesis, shown significantly higher florescence intensity (Figure 2.5E). The florescence AGEs could be responsible for the inhibitory effect.

Then I checked osteoclastic marker gene expression by RT-PCR and found that glycated-HSA significantly inhibited TRAP, CTSK, MMP9 mRNA expression, but did not change Atp6v, and receptor RAGE (Figure 3.1A) that shows glycated-HSA inhibited osteoclastogenesis by all means, differentiation, and activation.

Next I checked early osteoclastogenic and fusion related markers like TRAF-6, Integrin β3, DC-STAMP, OC-STAMP [1,17,33,51,52] after 1, 2 and 3 days, but none of the glycated-HSA showed any effect on these gene expression (Figure 3.1B). As glycated-HSA previously reported to induce inflammatory and osteoclastogenic cytokine TNFα, IL-1β, IL-6 production [19], therefore, we checked these cytokine mRNA expression in our osteoclastogenic culture condition. TNFα mRNA expression was increased at higher dose of both of the glycated-HSA, IL-1β was decreased by HSA-Glycol, but higher

concentration of HSA-Glycer didn't change, and IL-6 was inhibited by both of the glycated-HSA (Figure 3.1C).

We found HSA-AGEs to prevent late osteoclastogenesis (Figure 3.2A) as it reduced TRAP activity of 3 days RANKL-treated cells. However, RANKL+ HSA-AGEs treated cells rescued TRAP activity when the media was changed with RANKL alone after 3 days demonstrated that HSA-AGE treated cells have potential to rescue osteoclastogenesis upon AGE removal. This data shows that HSA-AGEs can alter late osteoclastogenesis. Glycated-HSA did not induce TRAP activity in the absence of RANKL.

In addition, none of the experimental conditions induced cell death except for HSA-AGEs in the absence of RANKL and the αMEM (Figure 3.2B), which could be due to excess growth as in rest of the conditions RANKL shifted to differentiation and thereby reduced cellular growth.

Non-histone nuclear protein High-mobility group box 1 (HMGB1), upon activation by RANKL, is released by macrophages into the extracellular environment and then bind with RAGE and play crucial role in both *in vivo* and *in vitro* osteoclastogenesis by regulating actin cytoskeleton reorganization [17]. In our study, cellular HMGB1 of RANKL-induced cells were not changed upon time, but secretion was induced time dependently and reached highest after 3 days of treatment. We had to renew culture media

after 3 days, so 4 days media did not shown HMGB1 (Figure 3.3A). To check HMGB1 secretion, we have chosen 3 days' time for rest of the experiments. As we found three bands of HMGB1, so we confirmed all of the bands were HMGB1 by siHMGB1 experiments as siHMGB1 downregulated all of the three bands in media, but not in cell lysate (Figure 3.3B). RAGE expression was induced by RANKL treatment and was highest after 18 h to 3 days, then decline, shows the role of RAGE in osteoclastogenesis (Figure 3.3A).

Next, I checked the effect of heated and glycated-HSA on HMGB1 and RAGE expression by the cell and HMGB1 secretion into media. I found that HMGB1 and RAGE expression were not changed in cell lysate by glycated-HSA (Figure 3.4A), but HMGB1 (25kDa) secretion falls down (Figure 3.4B). Therefore, I investigated whether glycated-HSA inhibition of HMGB1 secretion is dose dependent or not. I used glycated-HSA 150 and 500 μg/mL and found to decrease HMGB1 secretion was same, not dose dependent, it reached the level of no-RANKL treatment (Figure 3.4C-D). As HMGB1 is a multifunctional nuclear protein, I found it to be secreted in lower amount into culture media in the absence of RANKL (Figure 3.4C-D), but it did not induce osteoclastogenesis (Figure 2.5A, D). Therefore, we can conclude as the HMGB1 secreted upon RANKL-stimulation (not auto secretion as in the absence of RANKL) is playing crucial role in

osteoclastogenesis and glycated-HSA inhibited RANKL-induced HMGB1 secretion, thereby inhibited osteoclastogenesis.

As I found glycated-HSA to inhibit HMGB1 secretion, next I checked the effect of glycated-HSA on HMGB1 translocation from nucleus to cytoplasm to see if glycated-HSA inhibits translocation. HMGB1 originally located into nucleus and after certain stimulations, it translocate into cytoplasm (Figure 3.5A (0h)). In cytoplasmic fractions, HMGB1 and RAGE was not changed by glycated-HSA (Figure 3.5A-C). In nuclear fractions, HMGB1 was reduced (Figure 3.5A, D-E) by RANKL treatment shows the role of HMGB1 translocation in osteoclastogenesis. HMGB1 40 kDa and 25 kDa were significantly lowered by HSA-Glycol (Figure 3.5A, D-E). That shows HMGB1 translocation from nucleus to cytoplasm or re-translocation from cytoplasm to nucleus has been inhibited by glycated-HSA and that could be a possible reason of osteoclastogenesis inhibition.

NFκB, p38MAPK are known as osteoclastogenic pathway that directly induce osteoclastogenesis [2,22,31,53]. Glycated-HSA significantly inhibited NFκB activation (Figure 3.6A), but induced pERK phosphorylation after 30 and 60 min of treatment without causing any change on p38MAPK (Figure 3.6B). The MEK/ERK pathway was reported to suppress osteoclastogenesis in RAW264.7 cells [54]. In our experimental

conditions, glycated-HSA significantly induced pERK activation; it could be responsible to shift differentiation to proliferation as we found high cell growth (Figure 2.5C-D). Many studies show that pERK activation is critical for the fate of signal; it could lead differentiation, proliferation as well [54–57]. To investigate whether glycated-HSA stimulation of ERK activation is mediated through RAGE or not, we transfected RAW264.7 cells using siRAGE and then we used these cells to treat with glycated-HSA in the presence of RANKL. There we found ERK activation was significantly lowered by glycated-HSA, whereas, NFκB was not changed (Figure 3.7B). The effect of HSA-AGEs in differentiation pathway was altered in the presence of siRAGE shows the effect is seems to be RAGE dependent.

NFATc1 and c-Fos are major osteoclastogenic transcription factor [8,22,54]; therefore, we also investigated the effect of glycated-HSA and NFκB inhibitor on NFATc1 and c-Fos expression in RANKL-stimulated RAW264.7 cells by RT-PCR, and found to downregulate their expression (Figure 3.8). Glycated-HSA inhibited NFκB pathway (Fig. 3.7A) and NFATc1 and c-Fos (Figure 3.8) expression. NFκB inhibitor also inhibited NFATc1 and c-Fos (Figure 3.8) expression. siRAGE treatment did not alter NFκB pathway and inhibited excess ERK activation in response to glycated-HSA (Figure 3.7B). Taken together, the effect of HSA-AGEs are seems to be RAGE dependent.

RANKL-stimulation also induce Ca^{2+}-oscillation, and thereby induce NFATc1 and c-Fos to trigger osteoclastogenesis [33,55]. Therefore, I also investigated Ca^{2+}-oscillation in our experimental conditions and found glycated-HSA to significantly downregulate (Figure 3.9).

In this present study, I observed for the first time that glycation of HSA significantly downregulate osteoclastogenesis based on glycating agents used by downregulating RANKL-stimulated Ca^{2+}-oscillation, NFκB, NFATc1, c-Fos activation and HMGB1 secretion (Figure 3.10).

5 Conclusions

Firstly, I have established an in vitro osteoclastogenic model for RAW264.7 cell along with RANKL 100 ng/mL, 10% FBS, and cell density 10,000 cells/ well in 96-well plate. I used different osteoclastogenic maturation and activation markers such as TRAP staining, activity, multinucleated cell number, TRAP, CTSK, Atp6v, MMP9 mRNA expression. TRAP staining data was representative to TRAP activity, therefore, I used TRAP activity later on. Secondly, I found that glycated proteins significantly modulated RANKL-induced *in vitro* osteoclastogenesis in RAW264.7 cells both positively (collagen) and negatively (HSA) depending on the proteins and glycating agents used. RAGE expression was not changed in mRNA and protein level, but total osteoclastogenesis fall down by glycated-HSA, shows that the inhibitory effect is done after exposure to the RANKL and glycated-HSA; this inhibition does not need to downregulate RAGE expression. Finally, I found glycated-HSA inhibited RANKL-induced activation of calcium influx, NF-κB, master osteoclastogenic transcription factor NFATc1, c-Fos seems to act through RAGE, and the secretion of nuclear protein HMGB1 that plays major role in osteoclastogenesis. Macrophage cell also possess scavenger receptor class A I and II, scavenger receptor class B CD36 and SR-B1 that are known for uptake and removal of foreign matters such as modified low-density

lipoprotein, AGEs. Therefore, these receptors may play crucial role in response to different types of AGEs as HSA-Glu and HSA-Fru showed no effect.

A

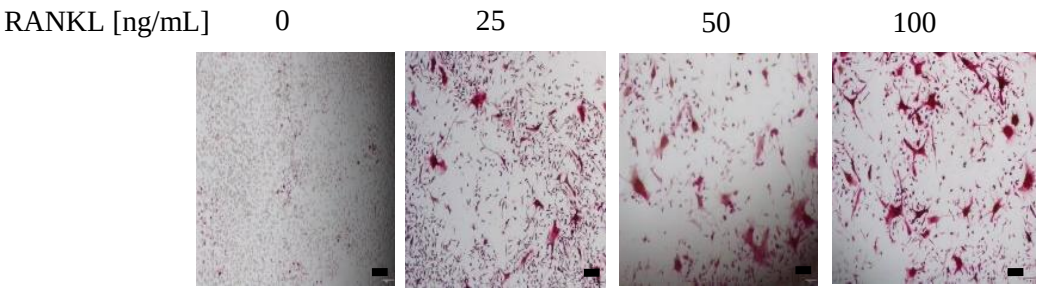
RANKL [ng/mL]
0
25
50
100

B

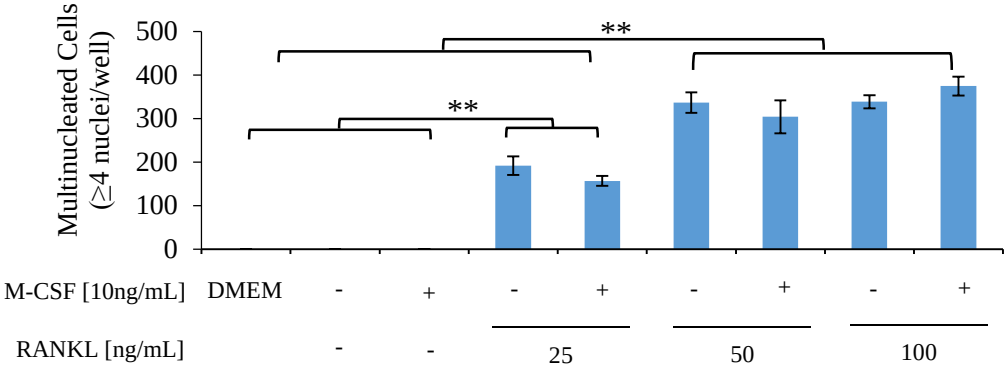
Multinucleated Cells
(≥4 nuclei/well)
500
400
300
200
100
0
**
**
M-CSF [10ng/mL]
DMEM
-
+
-
+
-
+
-
+
RANKL [ng/mL]
-
-
25
50
100

C

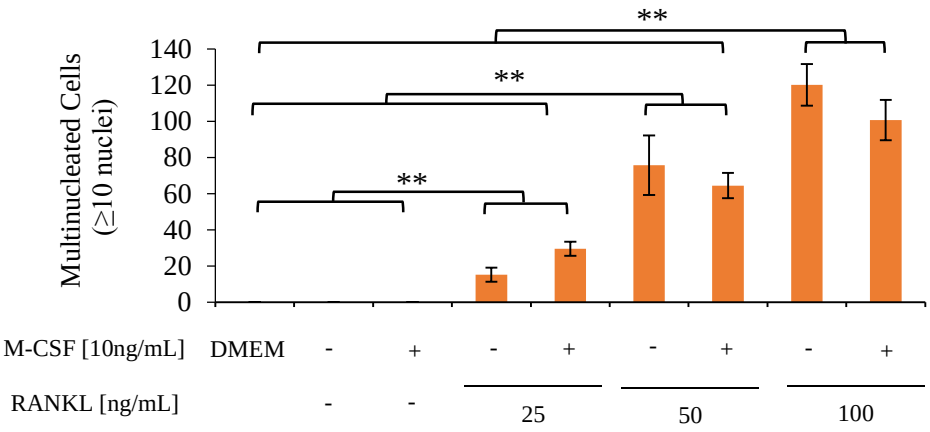
Multinucleated Cells
(≥10 nuclei)
140
120
100
80
60
40
20
0
**
**
**
M-CSF [10ng/mL]
DMEM
-
+
-
+
-
+
-
+
RANKL [ng/mL]
-
-
25
50
100

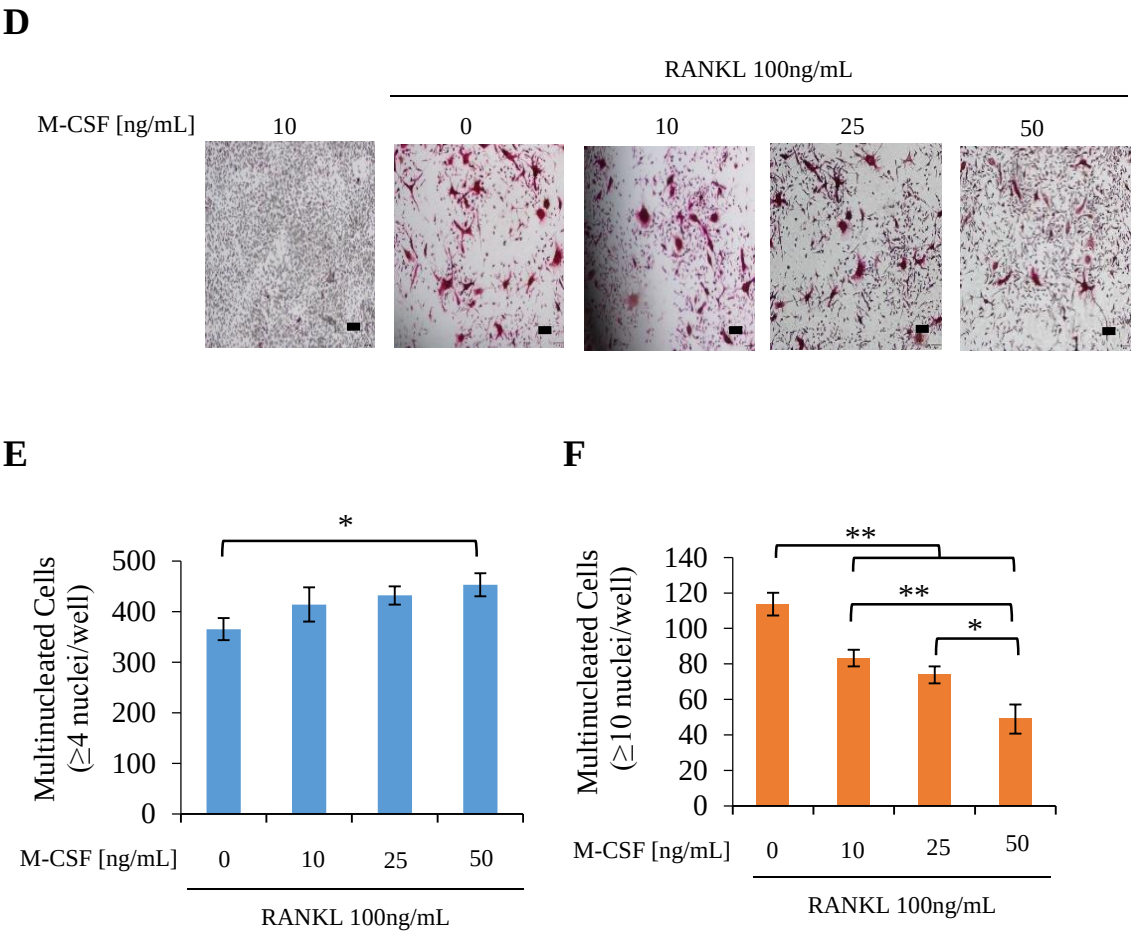

Figure 1.1: Effect of RANKL and M-CSF on osteoclastogenesis. RAW264.7 cells were treated with αMEM containing 10% FBS with the mentioned concentrations of RANKL with or without differing doses of M-CSF for 5 days. Microscopic observation of TRAP stained cells **A, D**, 100x magnification, the bar (▬) in each figure represents 100 µm. Multinucleated cells having ≥4 nuclei **B, E;** and ≥10 nuclei **C, F**). All data are shown as means ± SEM; n=6. Tukey-Kramer test. **: $p<0.01$, *: $p<0.05$.

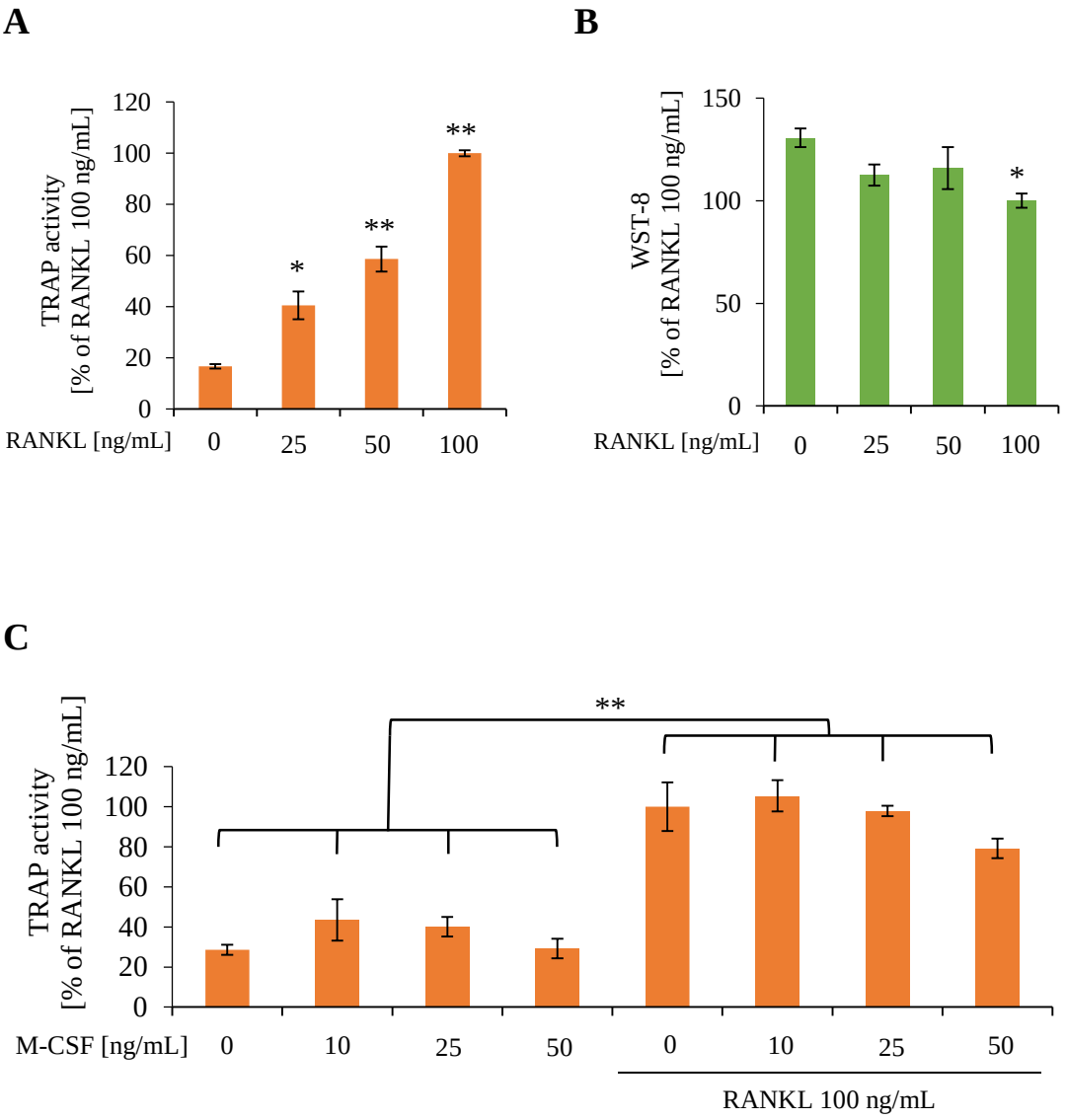
A
TRAP activity
[% of RANKL 100 ng/mL]
120
100
80
60
40
20
0
*
**
**
RANKL [ng/mL]
0
25
50
100
B
WST-8
[% of RANKL 100 ng/mL]
150
100
50
0
*
RANKL [ng/mL]
0
25
50
100
C
TRAP activity
[% of RANKL 100 ng/mL]
**
120
100
80
60
40
20
0
M-CSF [ng/mL]
0
10
25
50
0
10
25
50
RANKL 100 ng/mL

D

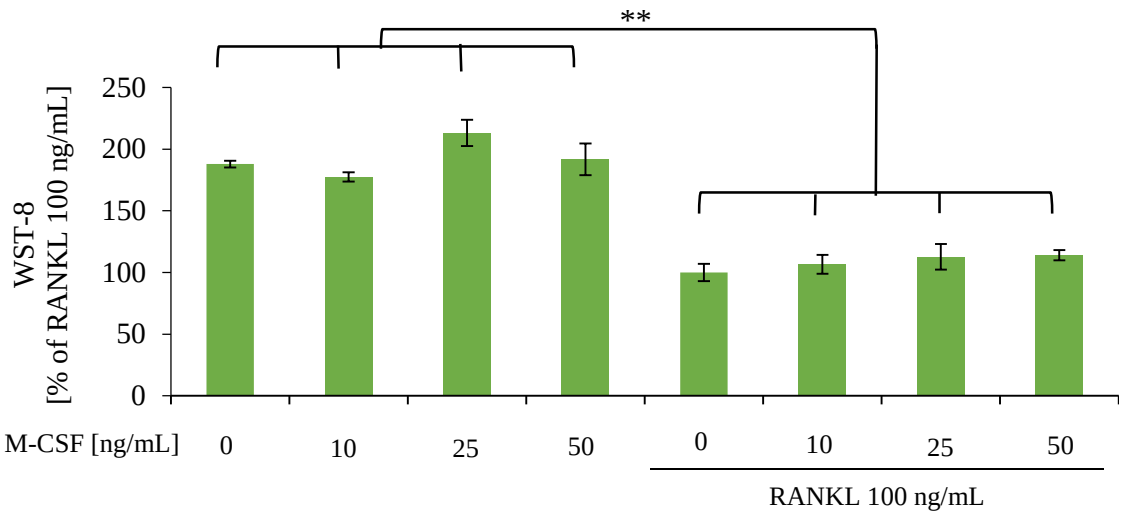

Figure 1.2: Effect of RANKL and M-CSF on TRAP activity and cell viability. A. Effect of RANKL (0 to 100 ng/mL) on TRAP activity, and B. WST-8 assay at day 5. C. Effect of M-CSF (0 to 50 ng/mL) with or without 100 ng/mL RANKL on TRAP activity, and D. WST-8 assay. Data are shown as mean ± SEM, n=3. Tukey-Kramer test. **: $p<0.01$, *: $p<0.05$.

A

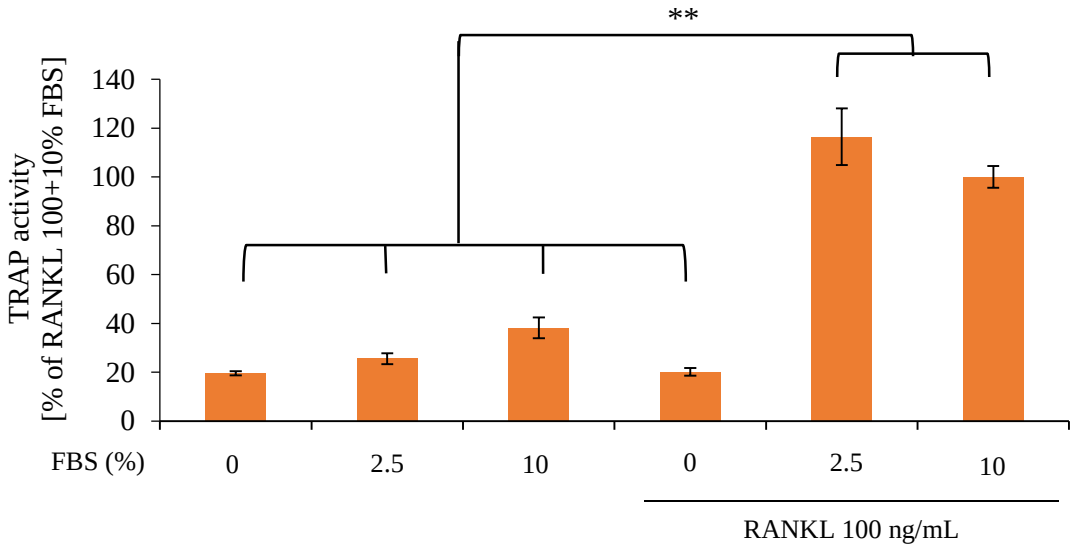

B

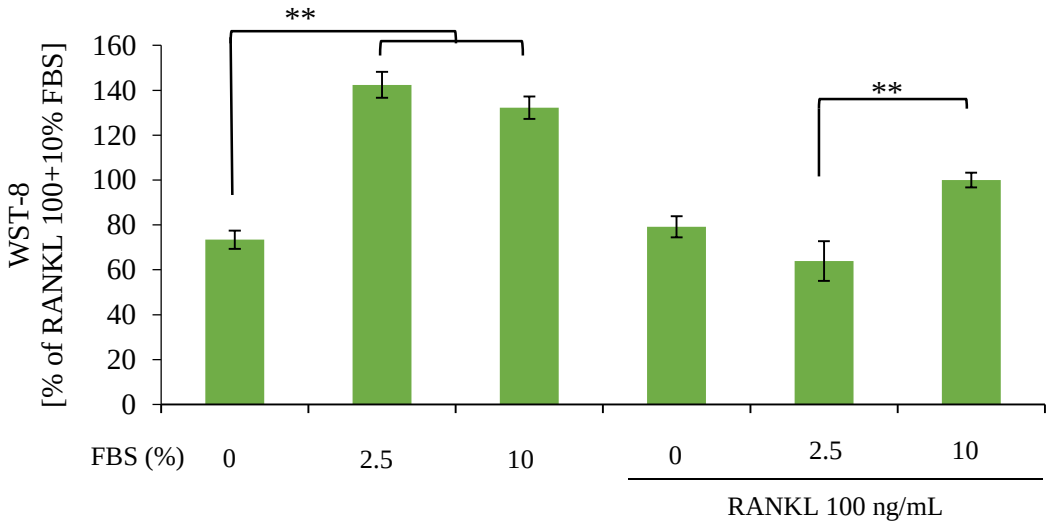

Figure 1.3: Effect of FBS on TRAP activity and cell viability. A. Effect of FBS on TRAP activity, and B. WST-8 assay at day 5. All data are as mean ± SEM, n=4. Tukey-Kramer test. **: $p<0.01$, *: $p<0.05$.

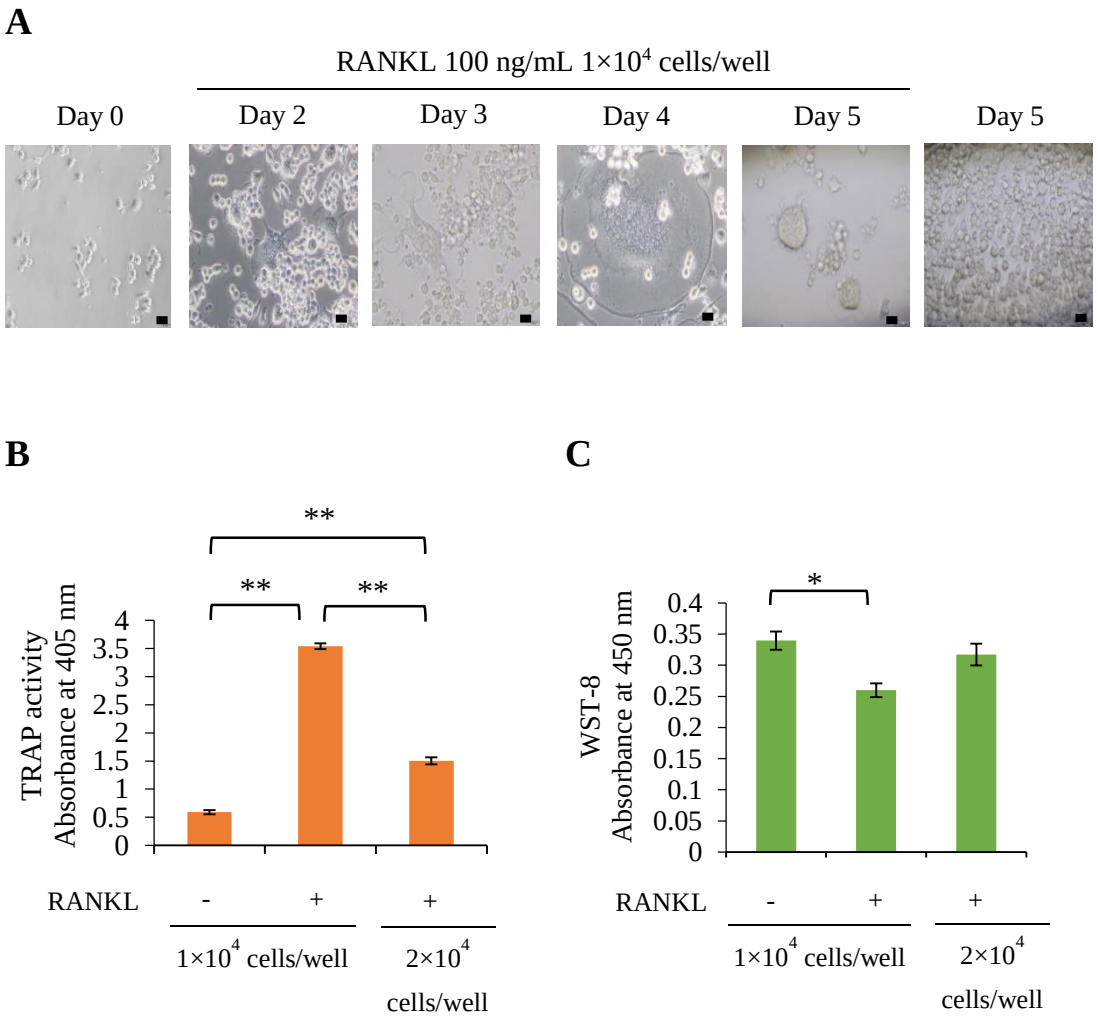

Figure 1.4: Effect of RAW264.7 cell number on osteoclastogenesis. A. RAW264.7 cells treated with RANKL 100 ng/mL was photographed using light microscope each day. The bar in each figure represents 20 µm. B. TRAP activity, and C. WST-8 assay at different cell density at day 5. All data are as mean ± SEM, n=3. Tukey-Kramer test. **: $p<0.01$, *: $p<0.05$.

A

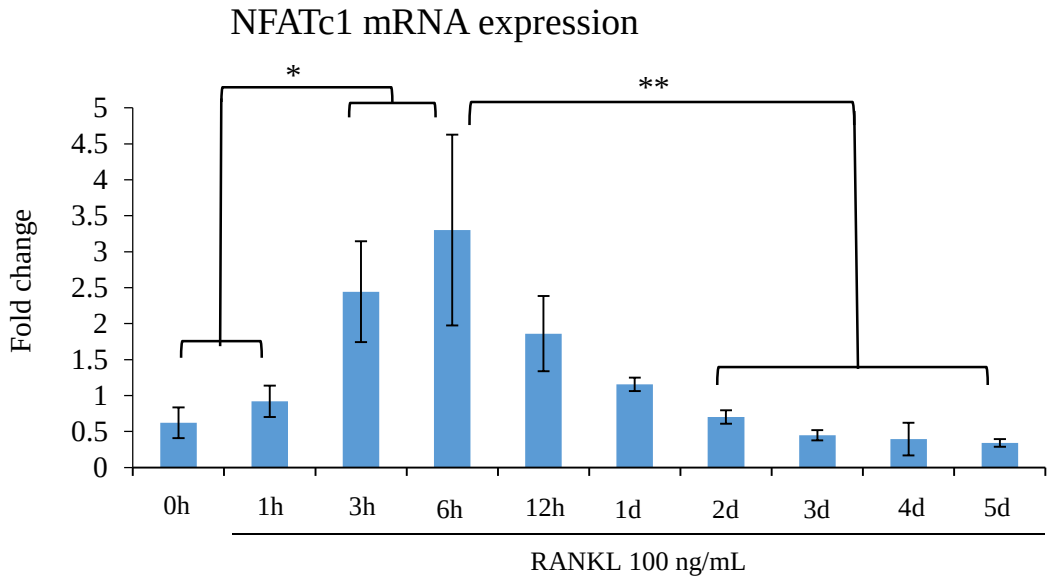

B

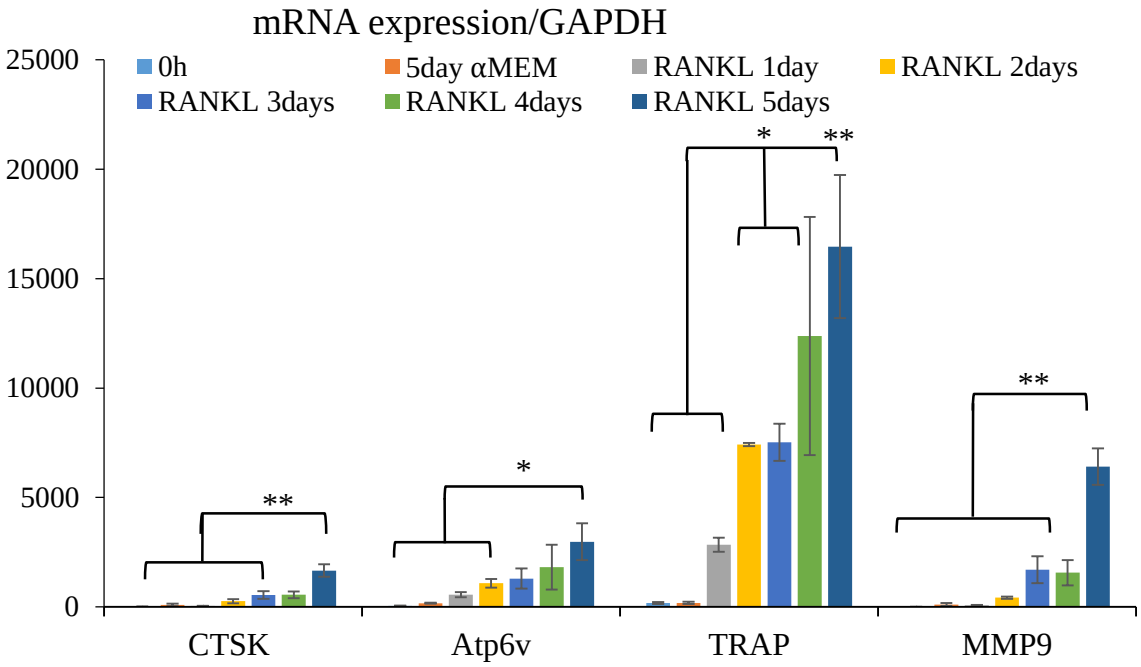

Figure 1.5: RANKL induced osteoclastogenic mRNA expression without M-CSF. RAW264.7 cells were plated in 24-well plates at 4×104 cells/well, and the next day cells were treated with αMEM containing 10% FBS without or with 100 ng/mL RANKL. After 3 days, the media was renewed. The treated cells were collected after the indicated times and mRNA was extracted. These were then used for cDNA synthesis and checked by RT-

PCR. Relative mRNA expression, data was normalized by GAPDH and showed as fold change. All data are shown as mean ± SEM, n=3. Tukey-Kramer test. **: $p<0.01$, *: $p<0.05$. A. NFATc1, B. CTSK, Atp6v, TRAP, MMP9.

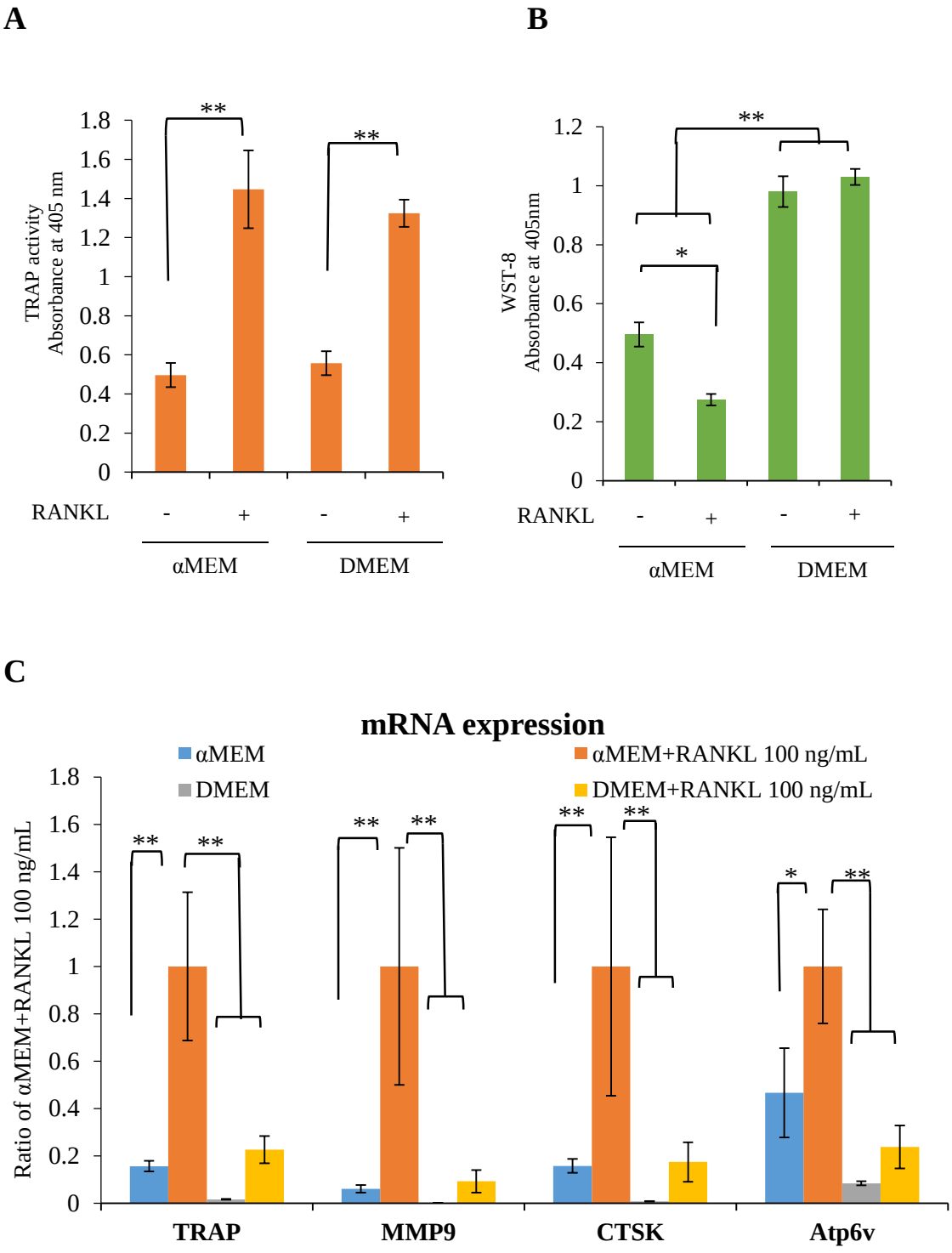

Figure 1.6: Effect of media on RANKL-induced osteoclastogenesis. RAW264.7 cells were plated in 24-well plates at 4×104 cells/well, and the next day cells were treated with αMEM or DMEM containing 10% FBS with or without 100 ng/mL RANKL. After 3 days, the media was renewed. At day 5, cells were used for A. Osteoclastogenic TRAP

activity assay, B. WST-8 assay, and C. RT-PCR analyses. Relative TRAP, MMP9, CTSK, Atp6v mRNA expression, data was normalized by GAPDH and shown as a fold change. All data are as mean ± SEM, n=3. Tukey-Kramer test. **: $p<0.01$, *: $p<0.05$.

A

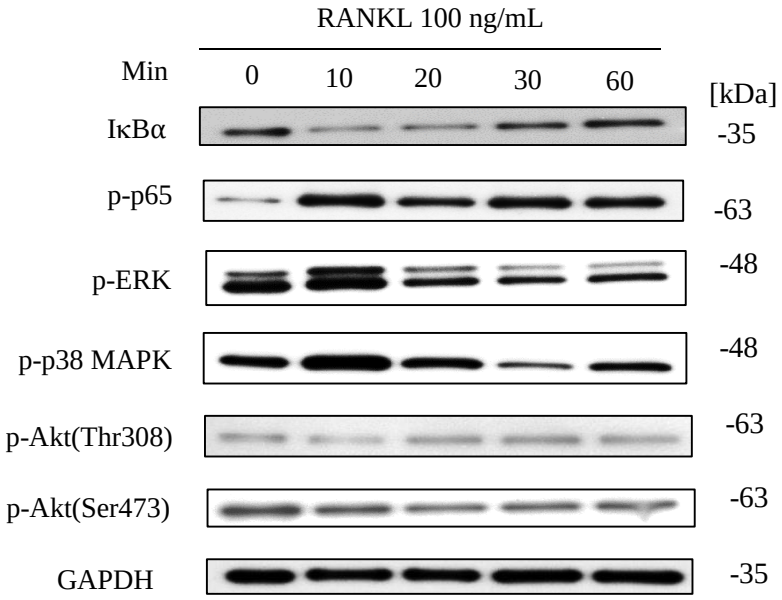

B

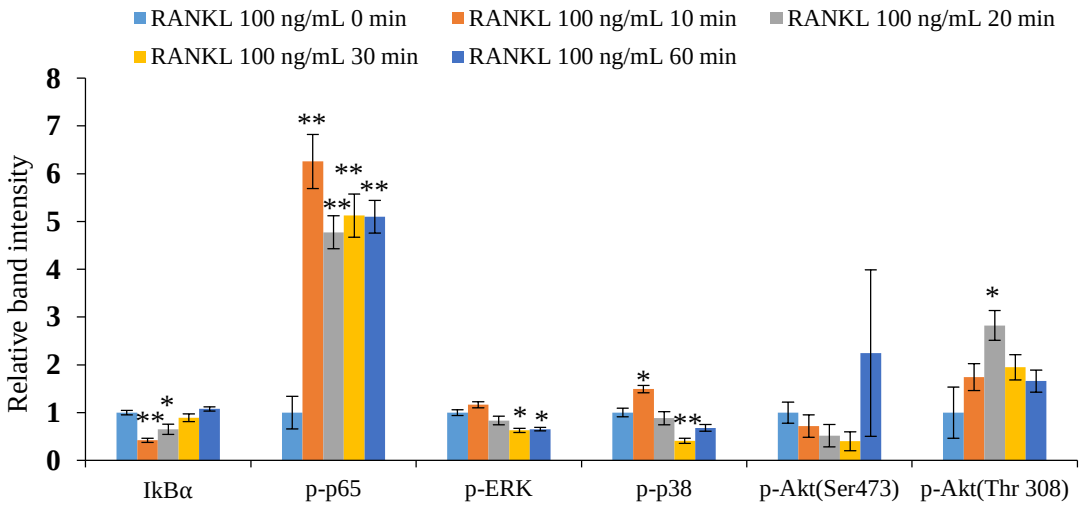

Figure 1.7: RANKL alone activated both osteoclastogenic and survival related pathways. A. RAW264.7 cells were plated in a 6-well plate at 2×10^5 cells/well, a followed by treatment with αMEM containing 10% FBS with 100 ng/mL RANKL the following day. After 0~60 min, the cells were collected and the cell lysates were prepared using RIPA buffer. Then 5 µg protein samples were used for western blot analysis using antibodies against the indicated proteins. B. ImageJ analysis of protein bands. Data were normalized by GAPDH and expressed as mean ± SEM, n=3. Tukey-Kramer test. ** $p<0.01$, * $p<0.05$.

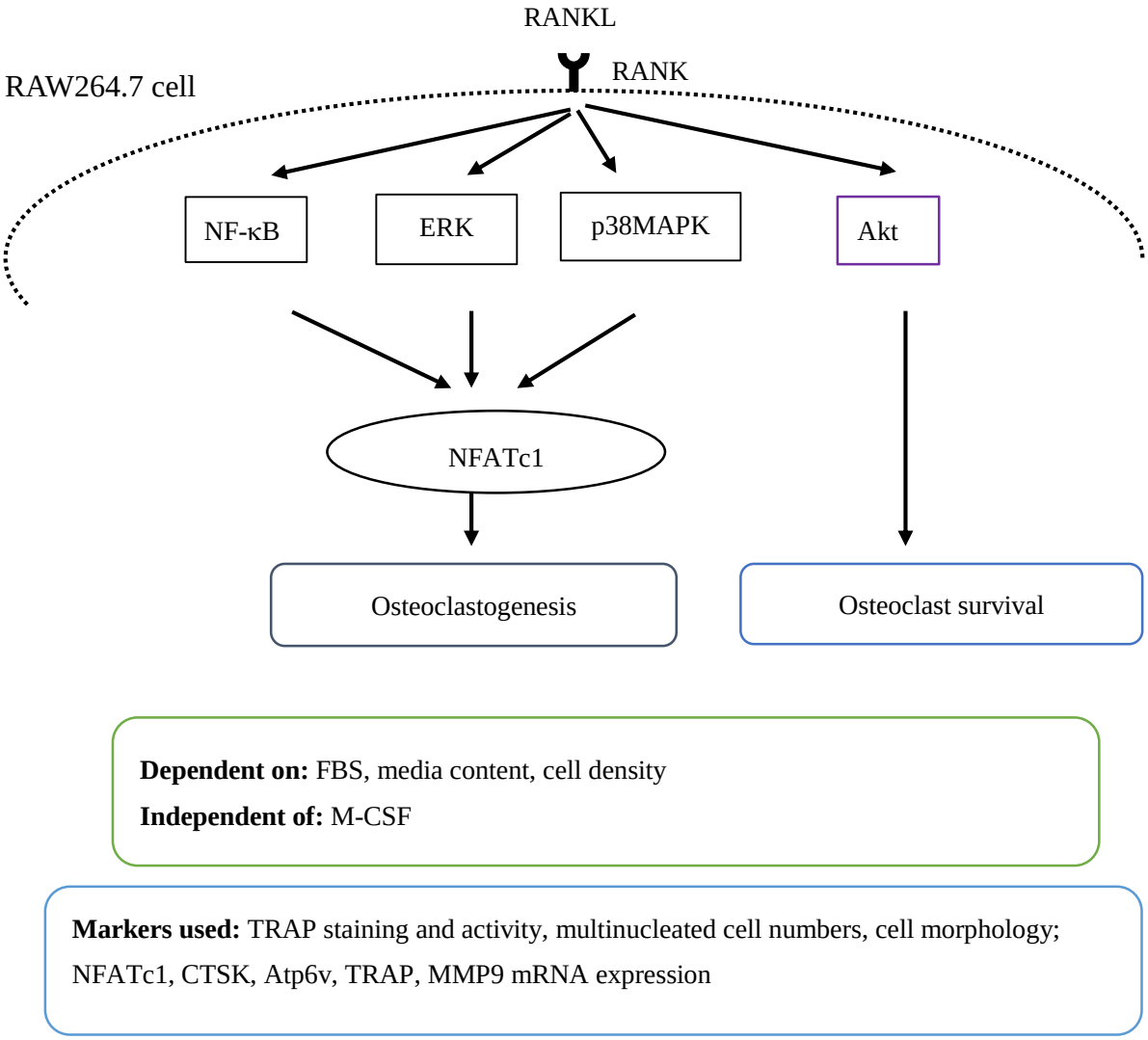

Figure 1.8: Schematic representation of RANKL-induced osteoclastogenesis in RAW264.7 cells.

A

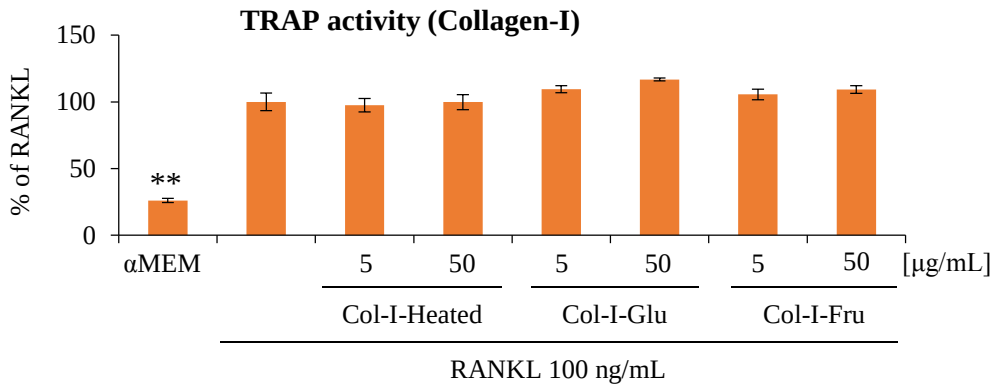

B

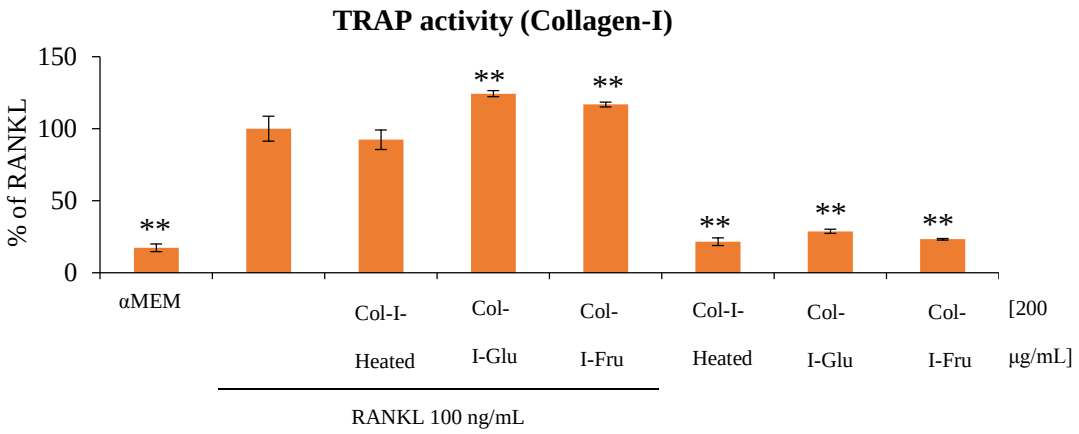

Figure 2.1: Effect of glycated Collagen-I on RANKL-induced osteoclastogenesis. RAW264.7 cells were treated with αMEM containing 10% FBS, 100 ng/mL RANKL with or without differing doses of collagen-I (heated, glycated) for 5 days. TRAP activity A, B. All data are shown as means ± SEM, n = 6. * $p < 0.05$, ** $p < 0.01$, Tukey-Kramer test.

A

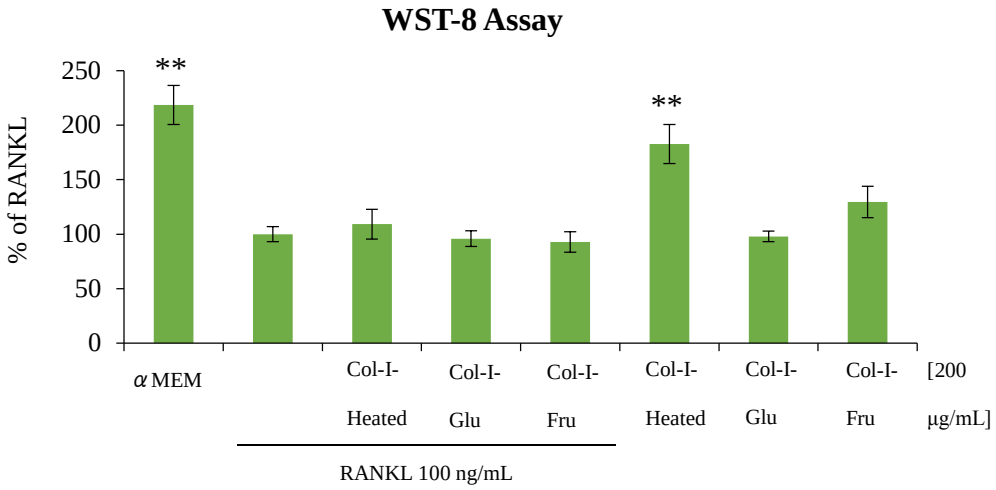

B

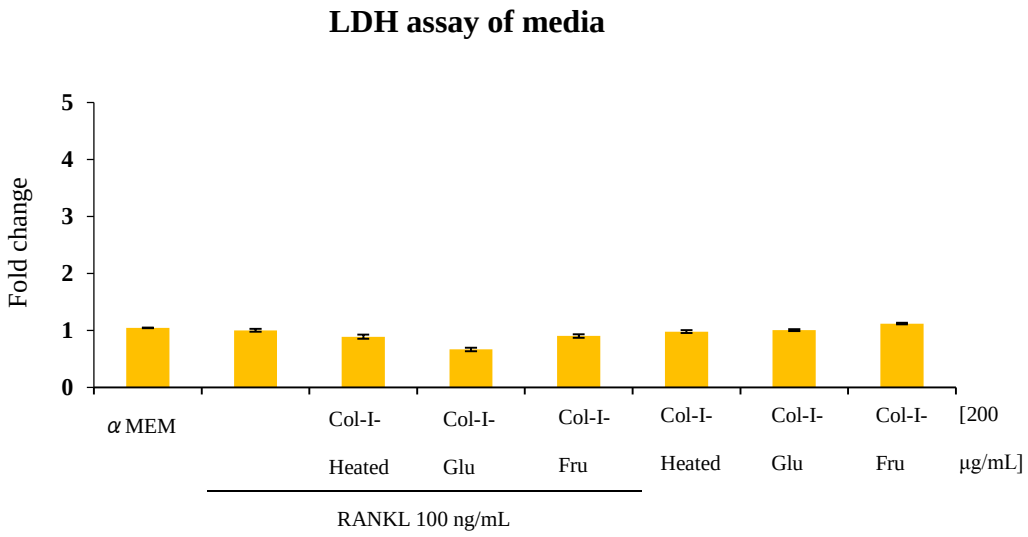

Figure 2.2: Effect of glycated Collagen-I on cell viability.

RAW264.7 cells were treated with αMEM containing 10% FBS, 100 ng/mL RANKL with or without differing doses of collagen-I (heated, glycated) for 5 days. WST-8 assay A, LDH secreted into media B. All data are shown as means ± SEM, n = 6. * $p < 0.05$, ** $p < 0.01$, Tukey-Kramer test.

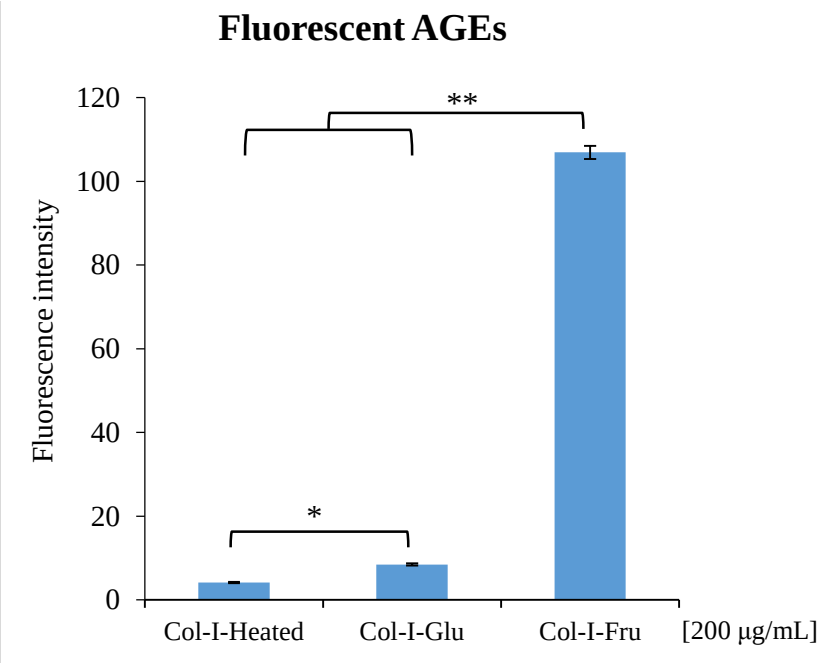

Figure 2.3: Fluorescent AGEs produced in glycation models.
Fluorescent intensity of glycated collagen-I. All data are shown as means ± SEM, n = 3. * $p < 0.05$, ** $p < 0.01$, Tukey-Kramer test.

A

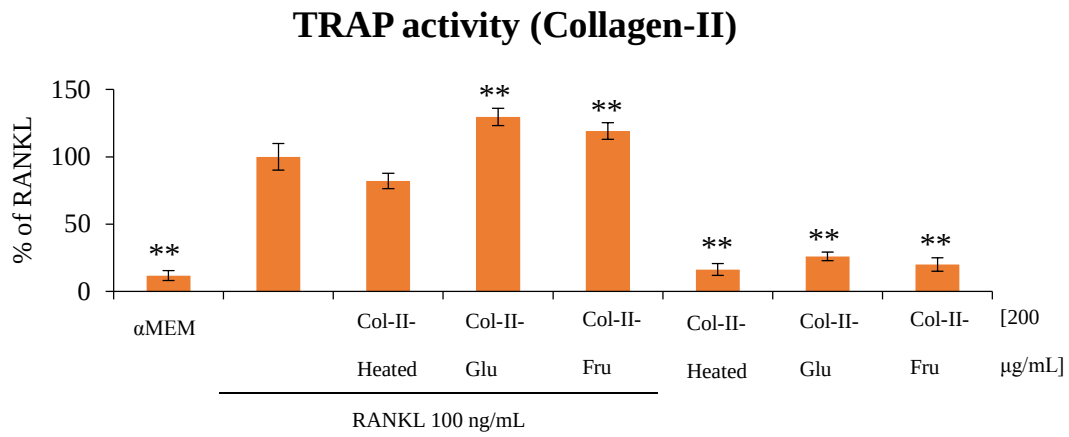

B

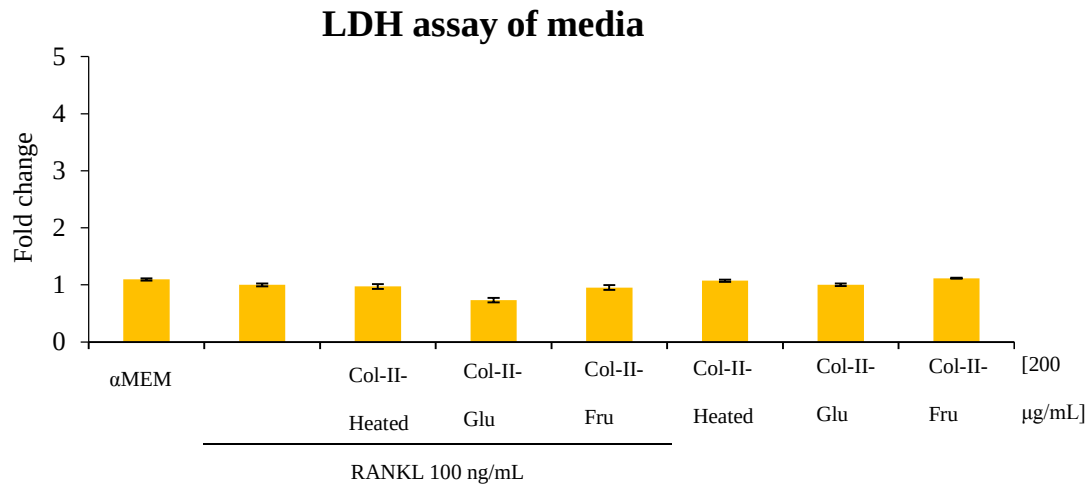

Figure 2.4: Effect of glycated Collagen-II on RANKL-induced osteoclastogenesis. RAW264.7 cells were treated with αMEM containing 10% FBS, 100 ng/mL RANKL with or without differing doses of collagen-II (heated, glycated) for 5 days. TRAP activity A; LDH secreted into media B. All data are shown as means ± SEM, n = 6. * $p < 0.05$, ** $p < 0.01$, Tukey-Kramer test.

A

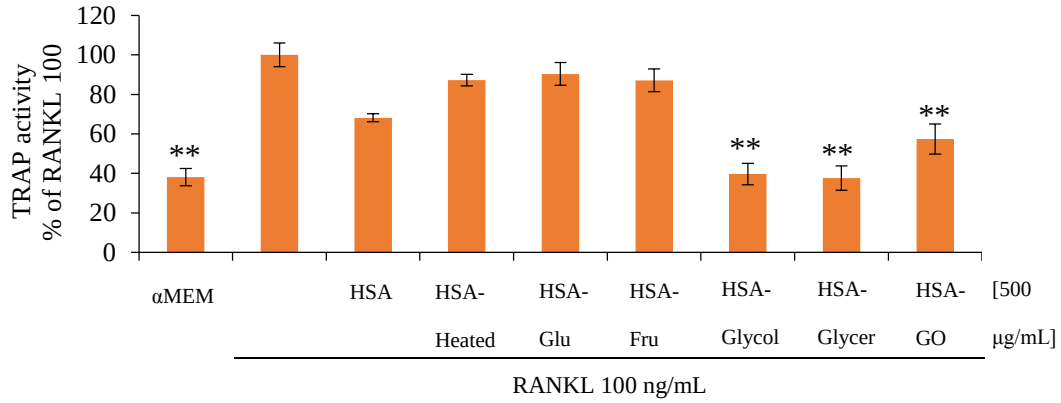
TRAP activity
% of RANKL 100
120
100
80
60
40
20
0
**
**
**
**
αMEM
HSA
HSA-Heated
HSA-Glu
HSA-Fru
HSA-Glycol
HSA-Glycer
HSA-GO
[500 μg/mL]
RANKL 100 ng/mL

B

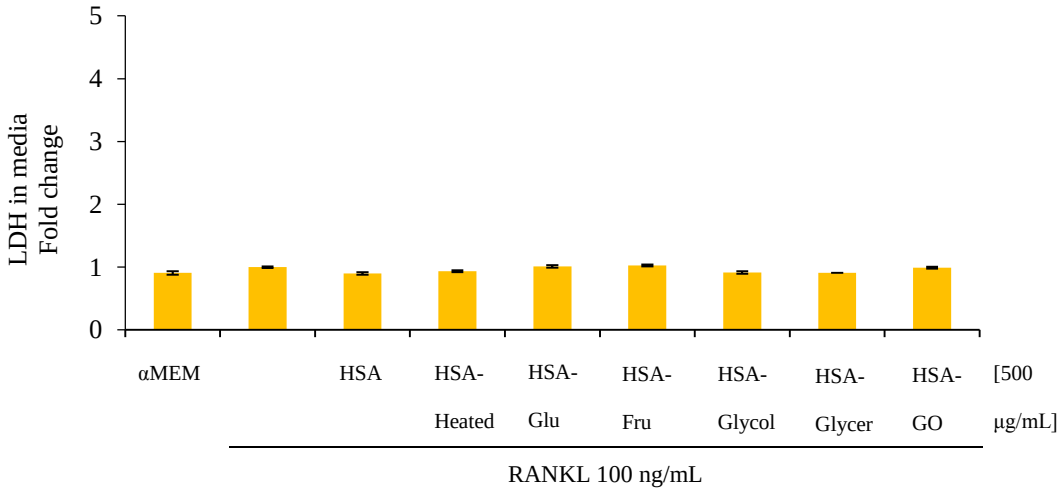
LDH in media
Fold change
5
4
3
2
1
0
αMEM
HSA
HSA-Heated
HSA-Glu
HSA-Fru
HSA-Glycol
HSA-Glycer
HSA-GO
[500 μg/mL]
RANKL 100 ng/mL

C

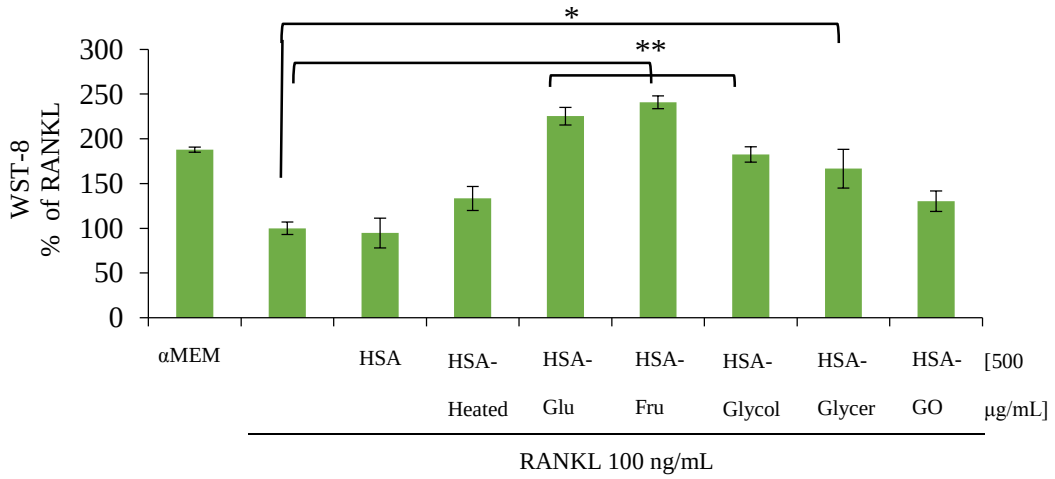
WST-8
% of RANKL
300
250
200
150
100
50
0
*
**
αMEM
HSA
HSA-Heated
HSA-Glu
HSA-Fru
HSA-Glycol
HSA-Glycer
HSA-GO
[500 μg/mL]
RANKL 100 ng/mL

D

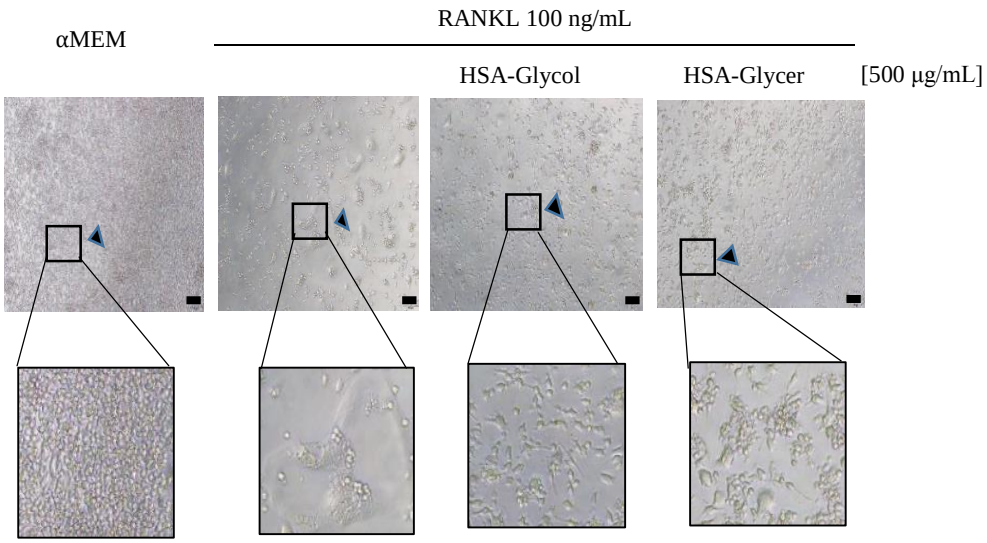

E

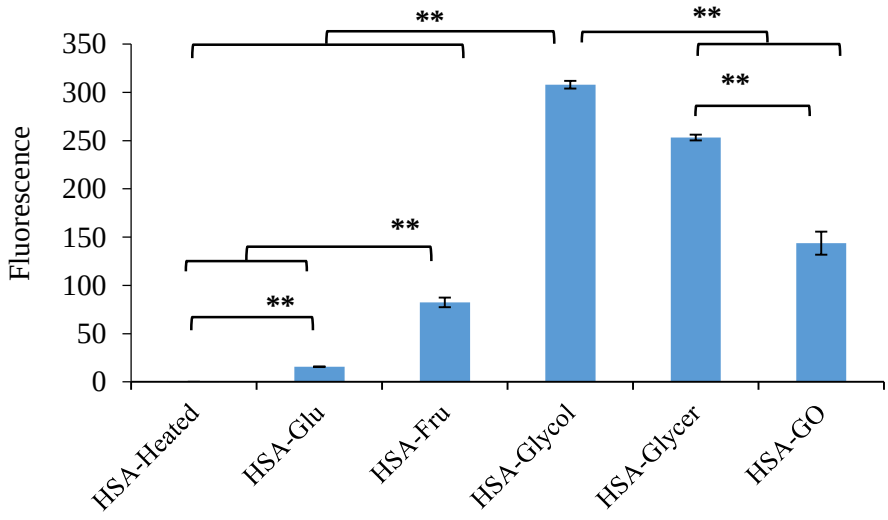

Figure 2.5: The effect of glycated-HSA on RAW264.7 cell osteoclastic differentiation. A. RAW264.7 cells were treated with HSA (native, heated, glycated) in the presence of RANKL for 5 days, and then TRAP activity was measured. B. LDH secreted into media by the same experimental cells. C. WST-8 assay of the cells treated with same conditions. Values are means ± SEM (n=6, each group). D. Morphology of the HSA-Glycol and HSA-Glycer treated osteoclast cell after 5 days of treatment. Bar (▬) represents 100μm. E. Fluorescence intensity of glycated-HSA 150μg/mL. Values are means ± SEM (n=3, each group), Tukey-Kramer test. **p<0.01, *p<0.05.

A

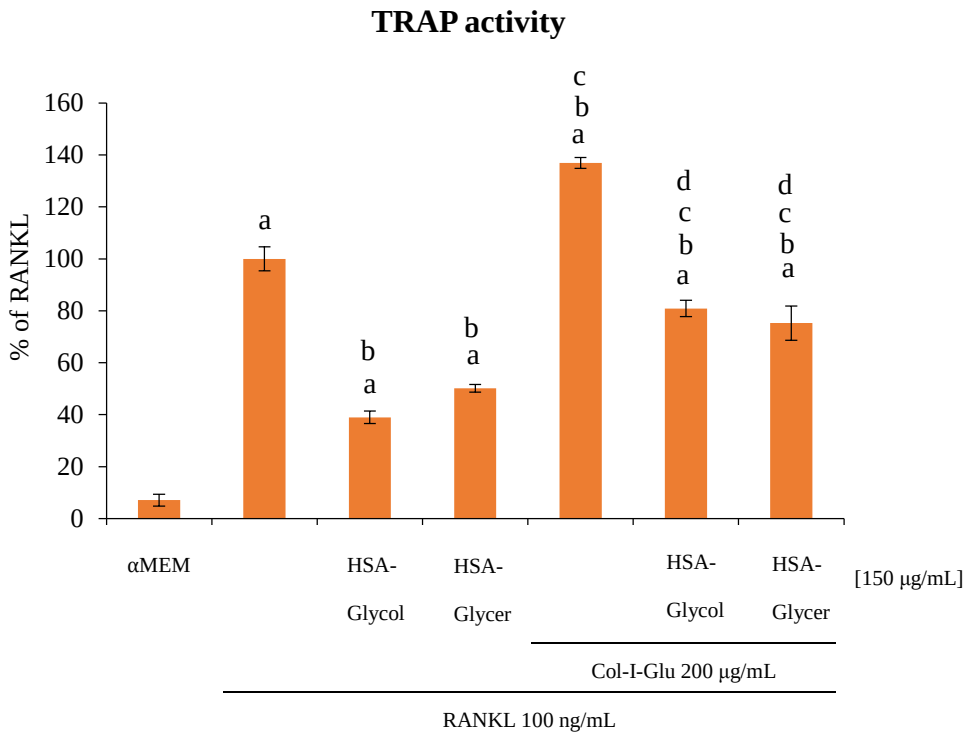

B

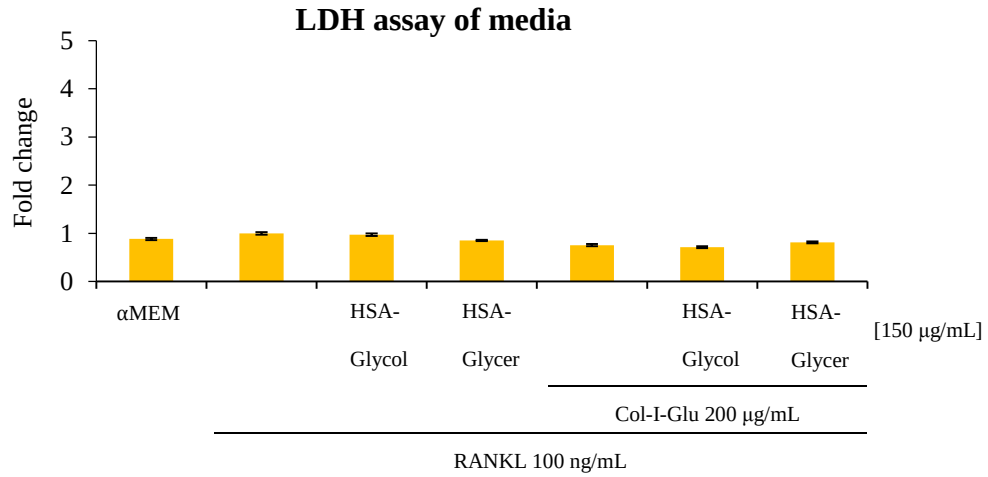

Figure 2.6: Effect of glycated collagen-I (Col-I-Glu) and HSA (HSA-Glycol, HSA-Glycer) together on osteoclastogenesis.

RAW264.7 cells were treated with RANKL 100 ng/mL along with Col-I-Glu in the presence and absence of HSA-Glycol or HSA-Glycer for 5 days and then TRAP activity was measured A. LDH assay of media B. All data are shown as means ± SEM, n = 6. Here, a, b, c, d ** $p < 0.01$ vs αMEM, RANKL, RANKL+Glycated-HSA, RANKL+Glycated-Collagen-I, respectively. Tukey-Kramer test.

A

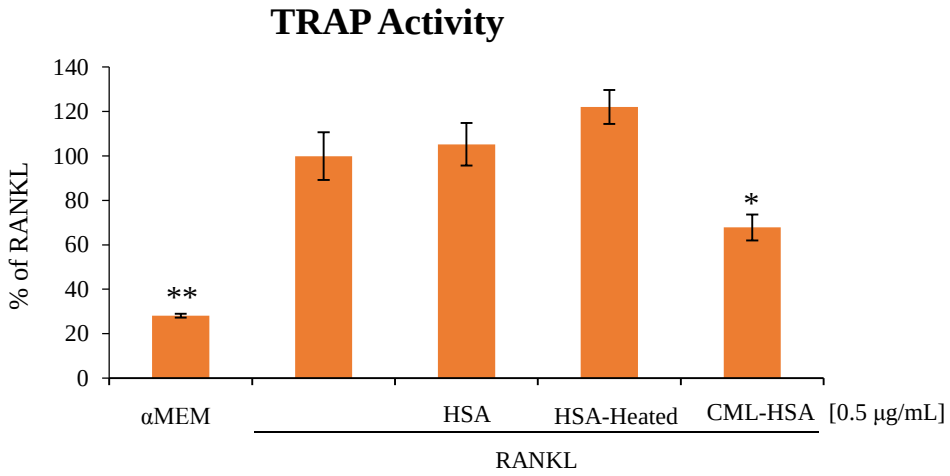

B

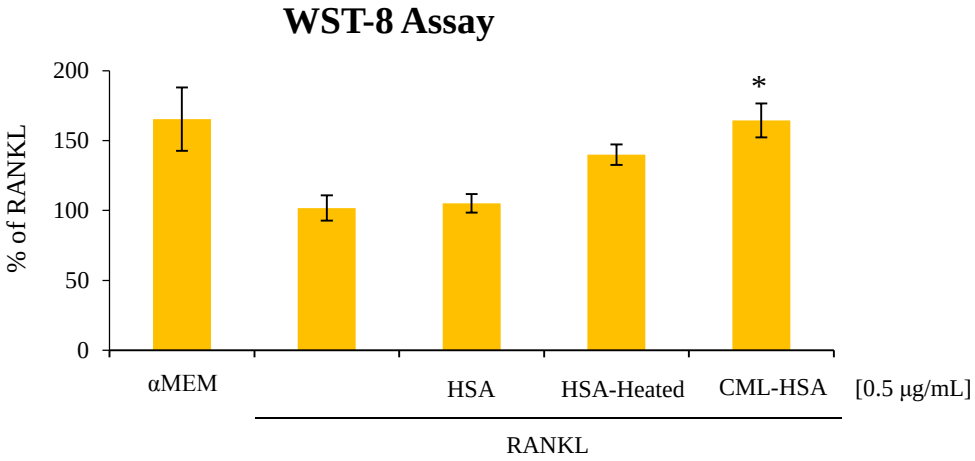

Figure 2.7: Effect of CML-HSA on osteoclastogenesis.
RAW264.7 cells were treated with αMEM containing 10% FBS, 100 ng/mL RANKL with or without HSA (native), HSA-heated, CML-HSA 0.5 µg/mL for 5 days and then TRAP activity was measured A. WST-8 assay B. All data are shown as means ± SEM, n = 3. * $p < 0.05$, ** $p < 0.01$, Tukey-Kramer test.

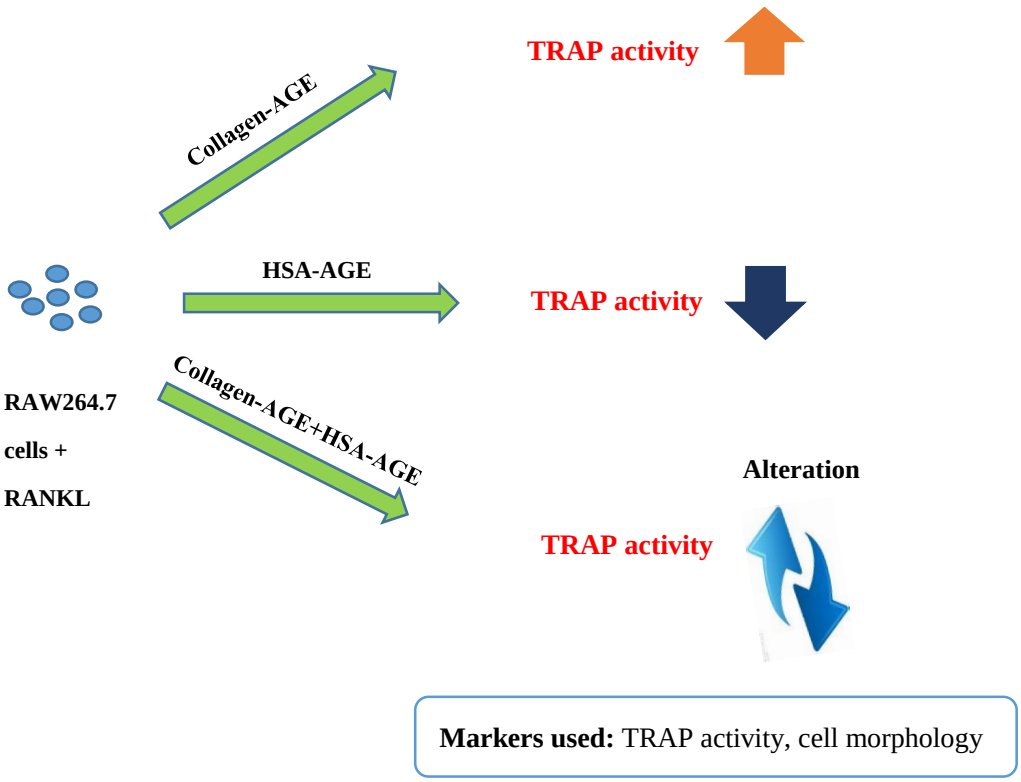

Figure 2.8: Schematic representation of effect of glycated proteins on RANKL-induced osteoclastogenic TRAP activity in RAW264.7 cells.

A

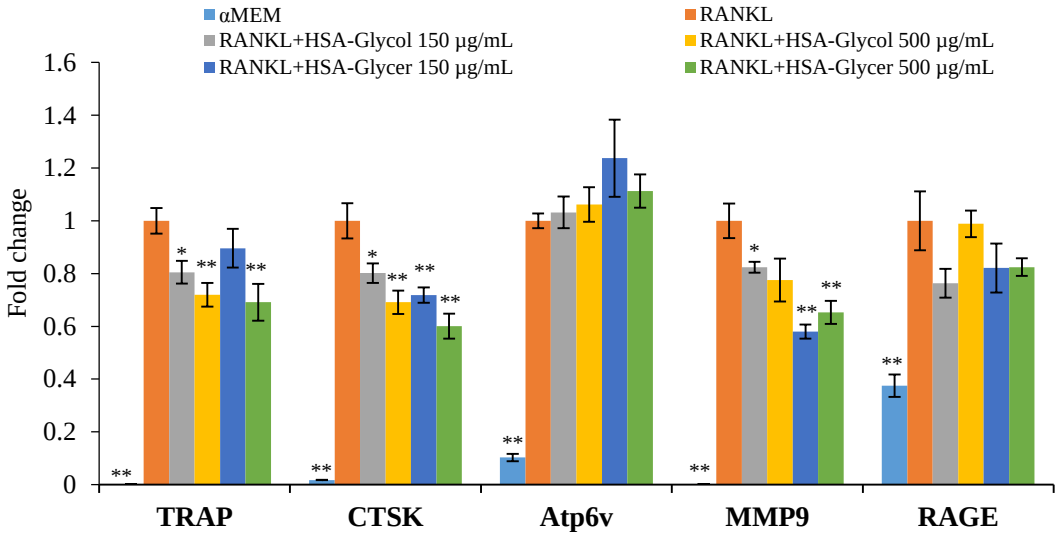
αMEM
RANKL
RANKL+HSA-Glycol 150 μg/mL
RANKL+HSA-Glycol 500 μg/mL
RANKL+HSA-Glycer 150 μg/mL
RANKL+HSA-Glycer 500 μg/mL
Fold change
1.6
1.4
1.2
1
0.8
0.6
0.4
0.2
0
TRAP
CTSK
Atp6v
MMP9
RAGE

B

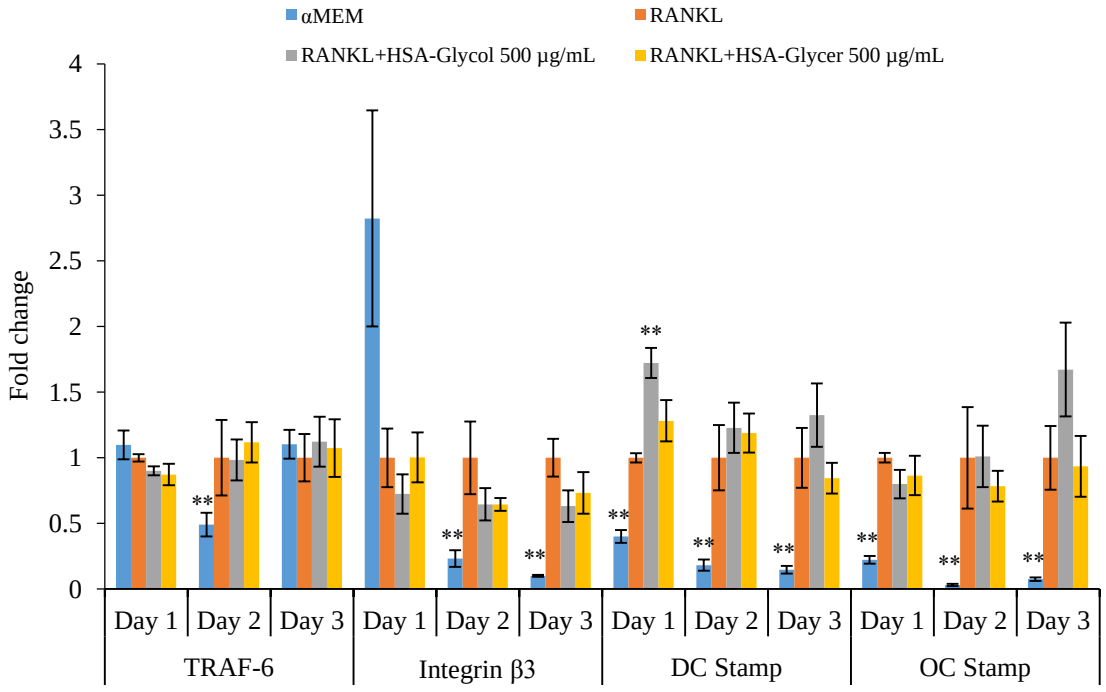
αMEM
RANKL
RANKL+HSA-Glycol 500 μg/mL
RANKL+HSA-Glycer 500 μg/mL
Fold change
4
3.5
3
2.5
2
1.5
1
0.5
0
Day 1
Day 2
Day 3
TRAF-6
Integrin β3
DC Stamp
OC Stamp

C

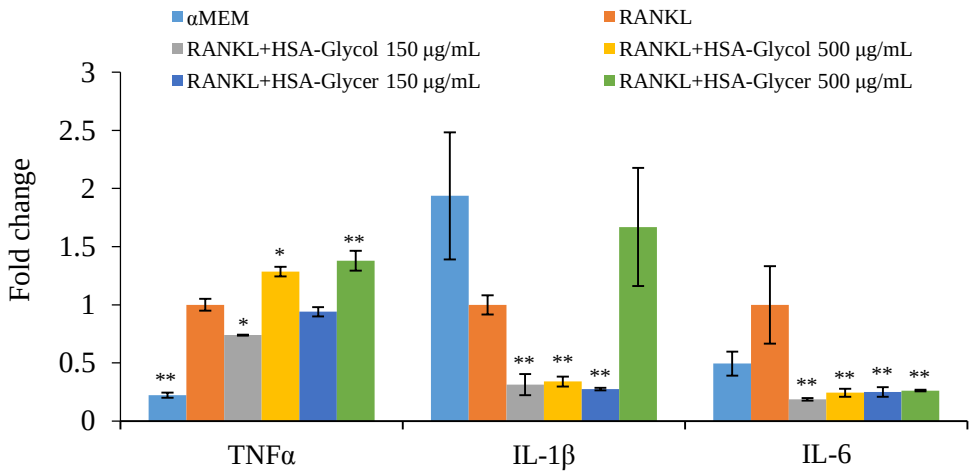

Figure 3.1: Glycated-HSA inhibited osteoclastogenic and inflammatory mRNA expression by RANKL-treated RAW264.7 cells.

A. RAW264.7 cells were treated with HSA (native, heated, glycated) in the presence of RANKL for 5 days, and then osteoclastic maturation marker TRAP, CTSK, Atp6v, MMP9, and RAGE mRNA expression was measured using RT-PCR. Values are means ± SEM (n=4, each group). Tukey-Kramer test. **p<0.01, *p<0.05 compared to RANKL. B. mRNA expression of early osteoclastogenic gene in RAW264.7 cells in different time points. Values are means ± SEM (n=4, each group). C. mRNA expression of inflammatory and osteoclastogenic cytokine TNFα, IL-1β, IL-6 after 6 h of treatment. Values are means ± SEM (n=3, each group).

A

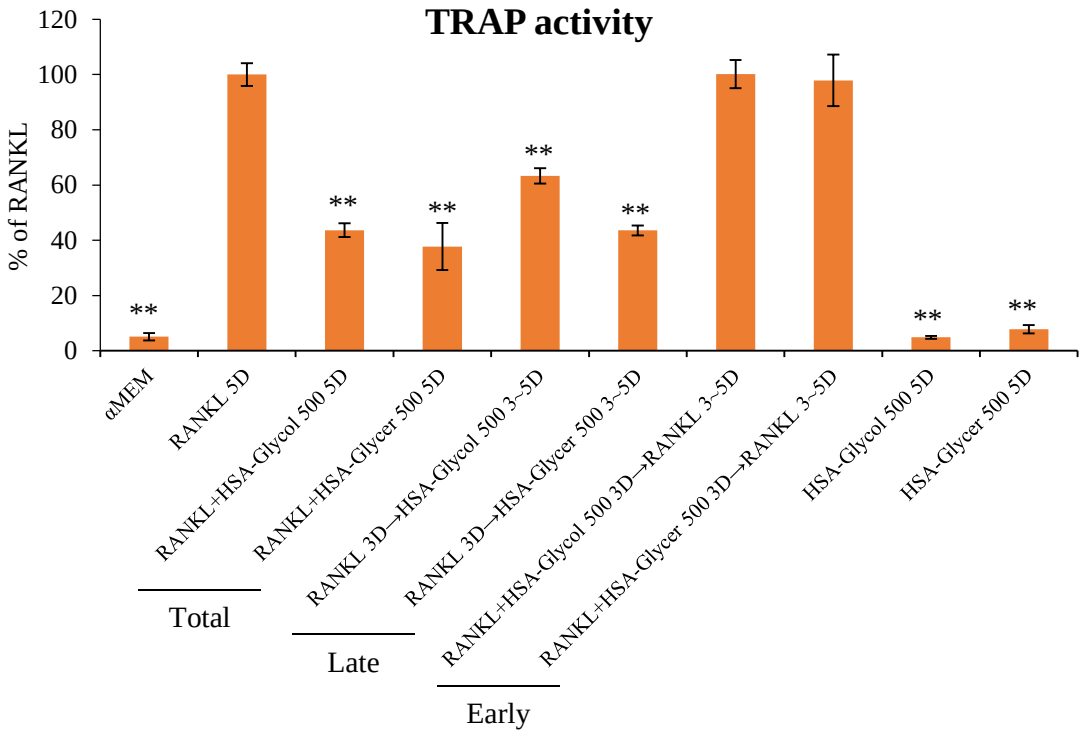
TRAP activity
% of RANKL
120
100
80
60
40
20
0
**
αMEM
RANKL 5D
RANKL+HSA-Glycol 500 5D
RANKL+HSA-Glycer 500 5D
RANKL 3D→HSA-Glycol 500 3~5D
RANKL 3D→HSA-Glycer 500 3~5D
RANKL+HSA-Glycol 500 3D→RANKL 3~5D
RANKL+HSA-Glycer 500 3D→RANKL 3~5D
HSA-Glycol 500 5D
HSA-Glycer 500 5D
Total
Late
Early

B

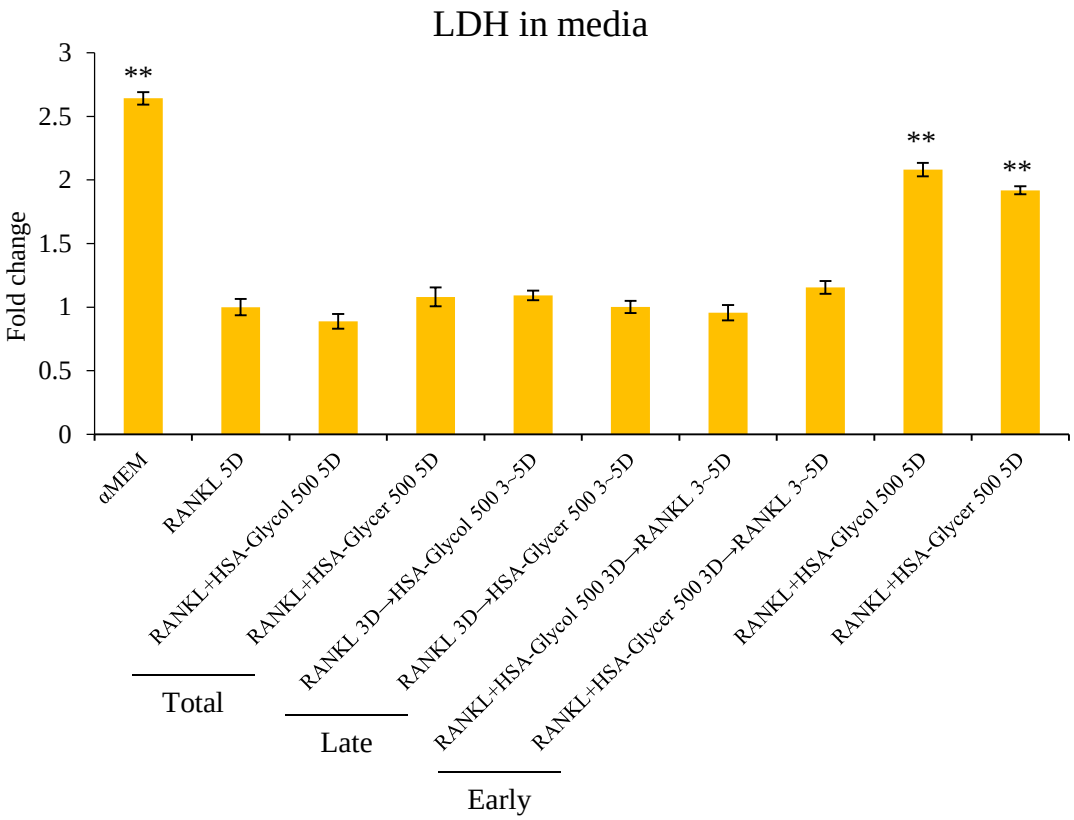

Figure 3.2: Effect of HSA-AGEs on osteoclastogenesis on early and later time point: A. HSA-AGEs significantly inhibited TRAP activity after 5 days. When RAW264.7 cells were treated with RANKL for 3 days and then media were replaced with RANKL+HSA-AGEs, TRAP activity were significantly inhibited compared to RANKL alone group. However, when RAW264.7 cells were treated with RANKL+HSA-AGEs for 3 days and then media were replaced with RANKL alone, TRAP activity was rescued as RANKL alone group. That shows RANKL+HSA-AGEs treated cells have potential to fuse and make osteoclast cells when HSA-AGEs are removed from the culture medium. HSA-AGEs alone did not induce TRAP activity. B. LDH activity of the media in same conditions after 5 days. Values are means ± SEM (n=6, each group). Tukey-Kramer test. **p<0.01, *p<0.05 compared to RANKL.

A

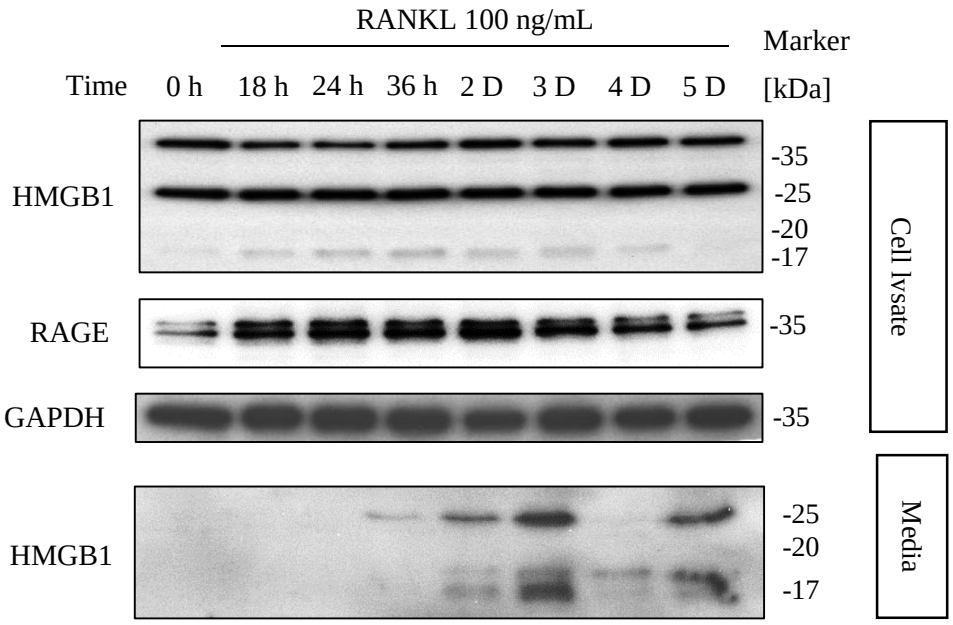

B

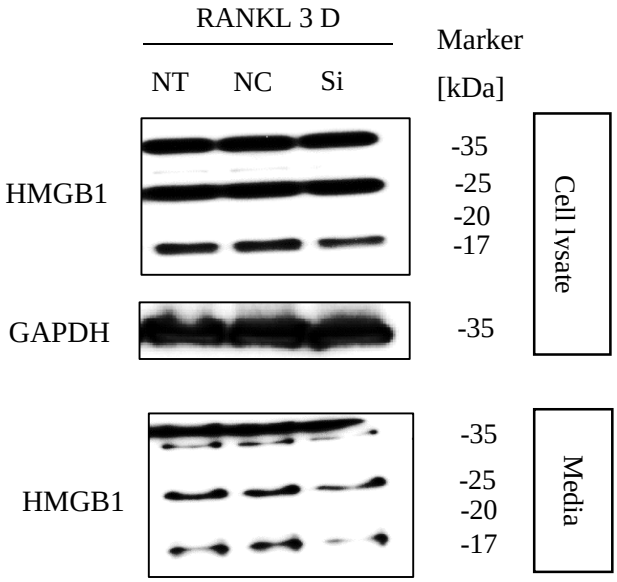

Figure 3.3: HMGB1 and RAGE protein expression upon RANKL treatment. A. RAW264.7 cells were treated with RANKL 100 ng/mL for indicated time and the expression of HMGB1, RAGE in cell lysate and the secretion of HMGB1 into media. B. RAW264.7 cells were transfected using siRNA for HMGB1 for 3 days and checked HMGB1 expression and secretion, n=3.

A

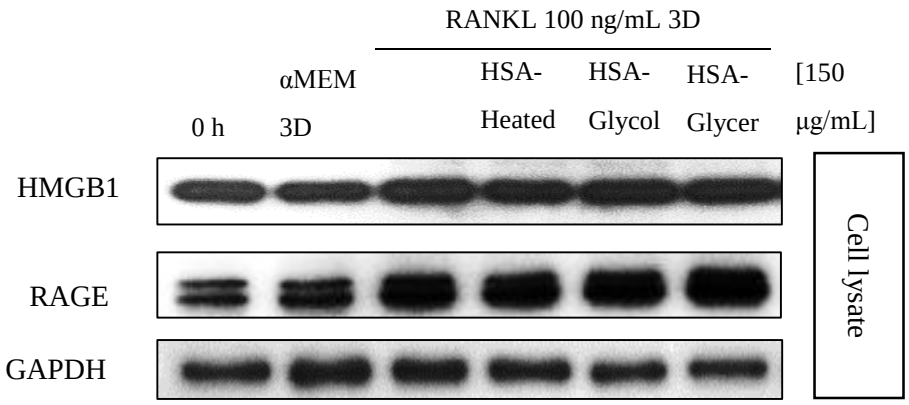
RANKL 100 ng/mL 3D
αMEM
HSA-
HSA-
HSA-
[150
0 h
3D
Heated
Glycol
Glycer
μg/mL]
HMGB1
RAGE
GAPDH
Cell lysate

B

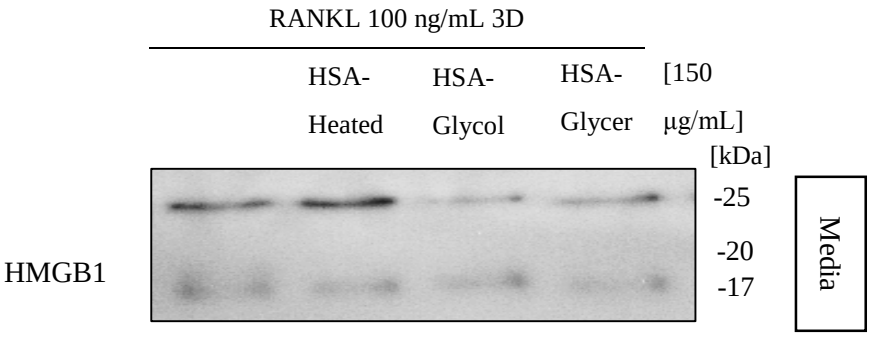
RANKL 100 ng/mL 3D
HSA-
HSA-
HSA-
[150
Heated
Glycol
Glycer
μg/mL]
[kDa]
-25
-20
-17
HMGB1
Media

C

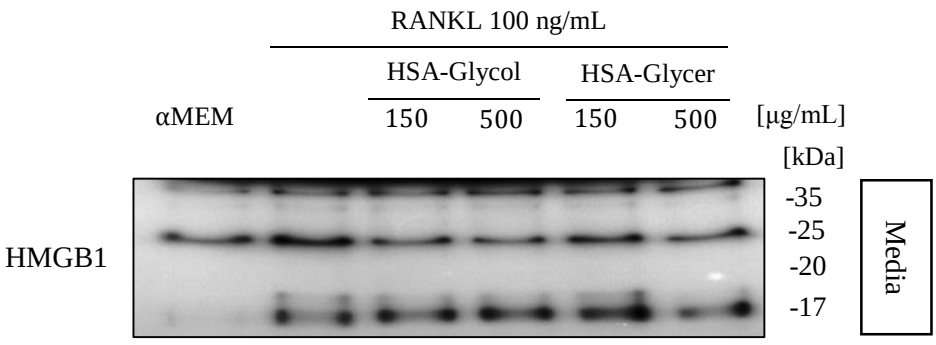
RANKL 100 ng/mL
HSA-Glycol
HSA-Glycer
αMEM
150
500
150
500
[μg/mL]
[kDa]
-35
-25
-20
-17
HMGB1
Media

D

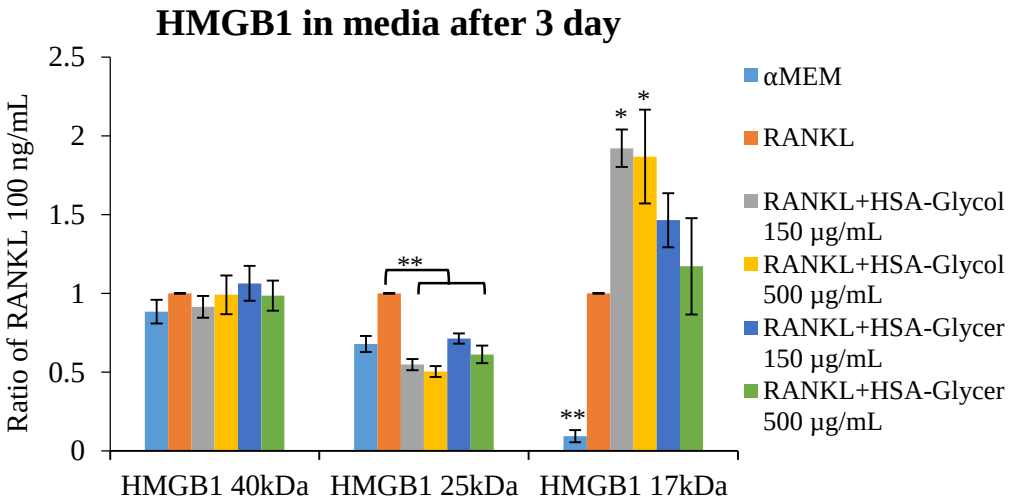

Figure 3.4. Effect of glycated-HSA on HMGB1 and RAGE protein expression. A. Effect of heated or glycated-HSA on RANKL-induced RAW264.7 cells after 3 days on HMGB1 and RAGE expression, n=3. B. HMGB1 secretion into media, n=3. C. HMGB1 secretion inhibition by glycated-HSA after 3 days of treatment, and D. ImageJ analysis of protein band intensity. Values are means ± SEM (n=11, each group), Tukey-Kramer test. **p<0.01, *p<0.05.

A

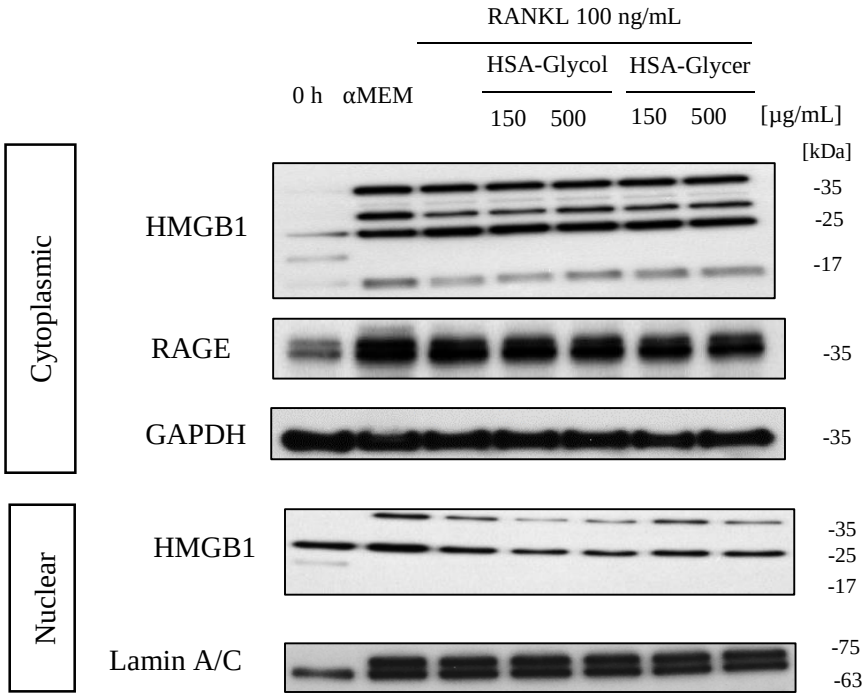
RANKL 100 ng/mL
HSA-Glycol
HSA-Glycer
0 h
αMEM
150
500
150
500
[μg/mL]
[kDa]
Cytoplasmic
HMGB1
-35
-25
-17
RAGE
-35
GAPDH
-35
Nuclear
HMGB1
-35
-25
-17
Lamin A/C
-75
-63

B

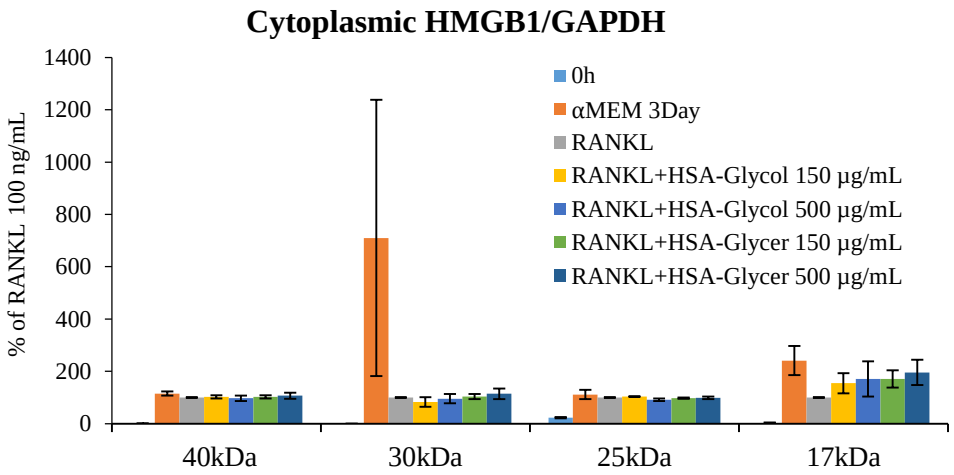
Cytoplasmic HMGB1/GAPDH
% of RANKL 100 ng/mL
1400
1200
1000
800
600
400
200
0
0h
αMEM 3Day
RANKL
RANKL+HSA-Glycol 150 μg/mL
RANKL+HSA-Glycol 500 μg/mL
RANKL+HSA-Glycer 150 μg/mL
RANKL+HSA-Glycer 500 μg/mL
40kDa
30kDa
25kDa
17kDa

C

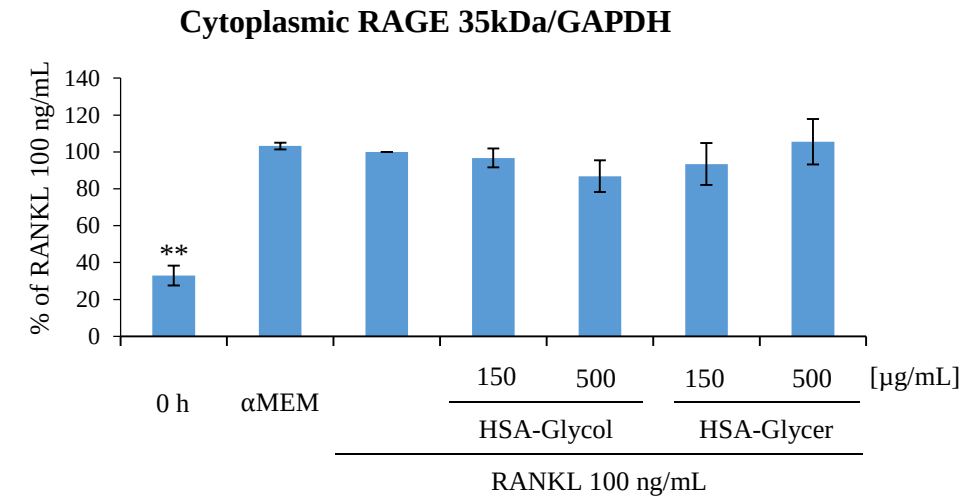
Cytoplasmic RAGE 35kDa/GAPDH
% of RANKL 100 ng/mL
140
120
100
80
60
40
20
0
**
0 h
αMEM
150
500
150
500
[μg/mL]
HSA-Glycol
HSA-Glycer
RANKL 100 ng/mL

D

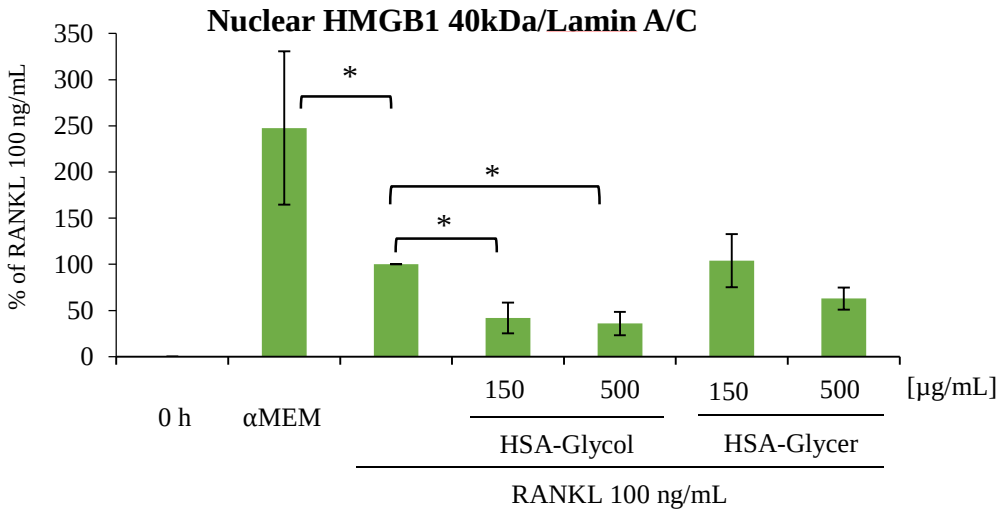
Nuclear HMGB1 40kDa/Lamin A/C
% of RANKL 100 ng/mL
350
300
250
200
150
100
50
0
*
*
*
0 h
αMEM
150
500
150
500
[μg/mL]
HSA-Glycol
HSA-Glycer
RANKL 100 ng/mL

E

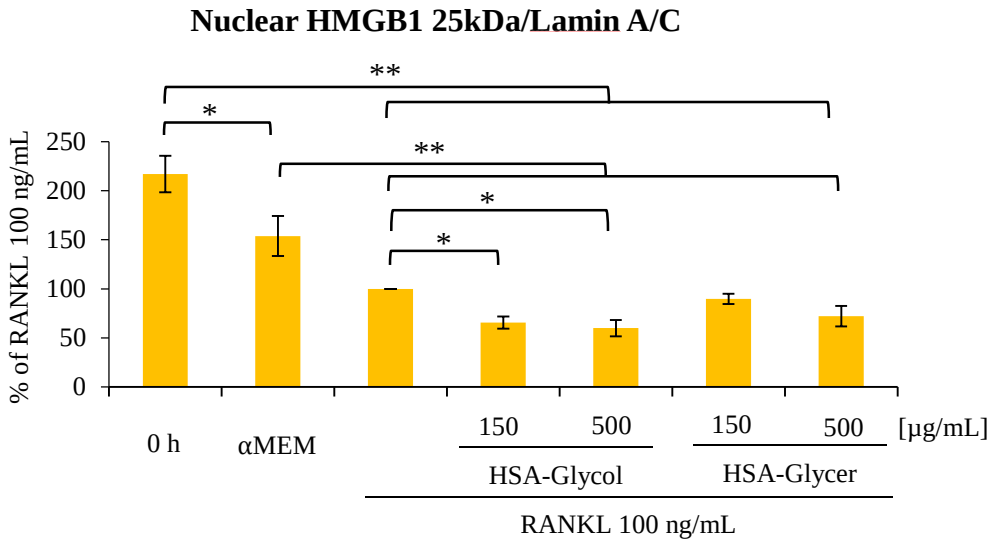

Figure 3.5: Cytoplasmic and nuclear translocation of HMGB1. A. RAW264.7 cells were treated with glycated-HSA in the presence of RANKL for 3 days and the cell protein were fractionated using nuclear and cytoplasmic extraction kit and then these were checked by western blot for HMGB1, RAGE, GAPDH, Lamin A/C. ImageJ analysis of the band intensity, B. Cytoplasmic HMGB1/GAPDH, C, Cytoplasmic RAGE/GAPDH, D. Nuclear HMGB1 40kDa/lamin A/C, E. Nuclear HMGB1 25kDa/lamin A/C. Values are means ± SEM (n=3, each group), Tukey-Kramer test. **p<0.01, *p<0.05.

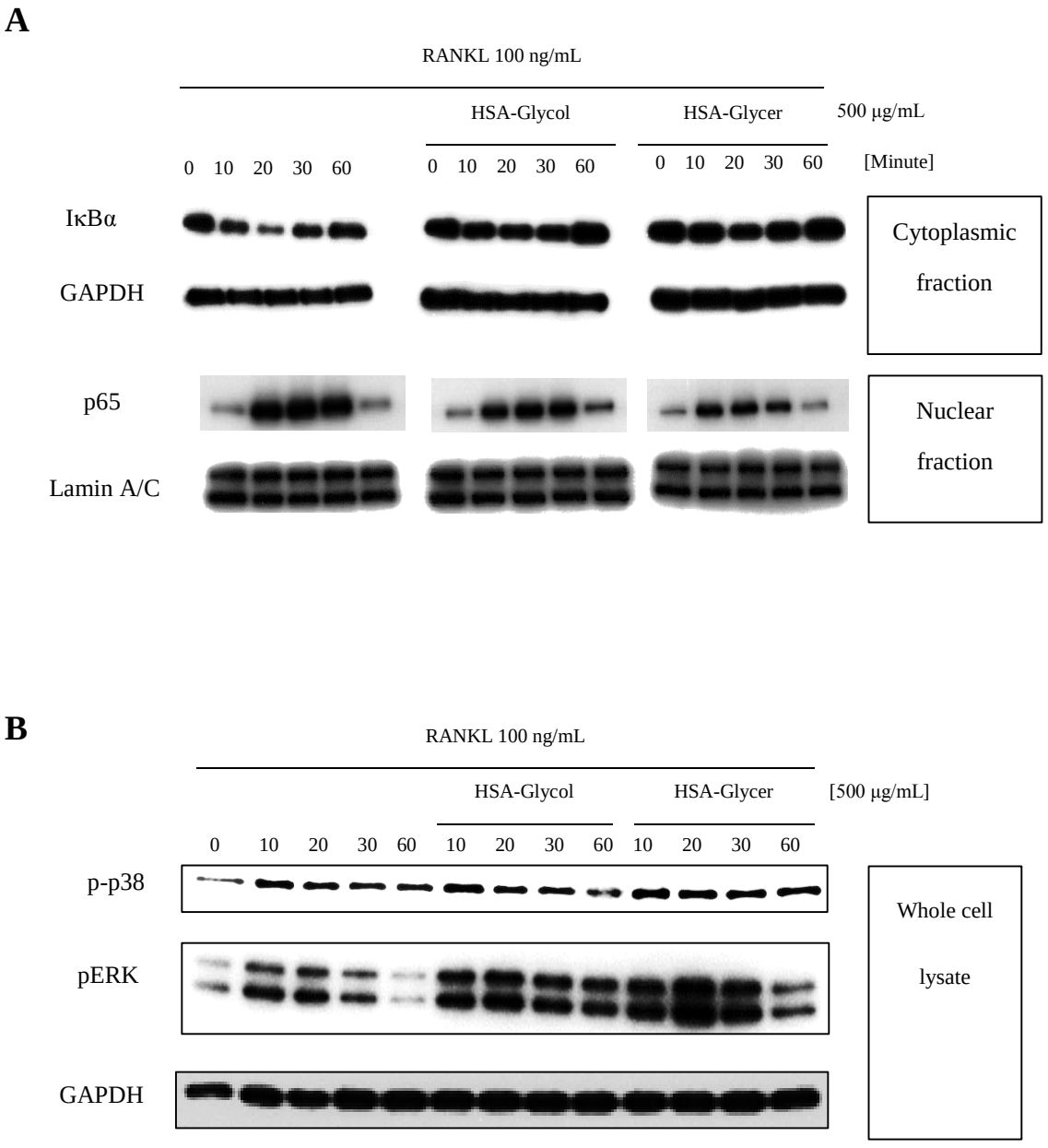

Figure 3.6: Effect of glycated-HSA on osteoclastogenic pathway activation. A. NFκB activation by experimental conditions. Cytoplasmic extracts were used for IκBα and nuclear extract were used for p65 detection by western blot. ImageJ analysis of band intensity. B. p38MAPK and pERK activation by experimental conditions in whole cell lysate and imageJ analysis of band intensity. Results are representative of three individual experiments.

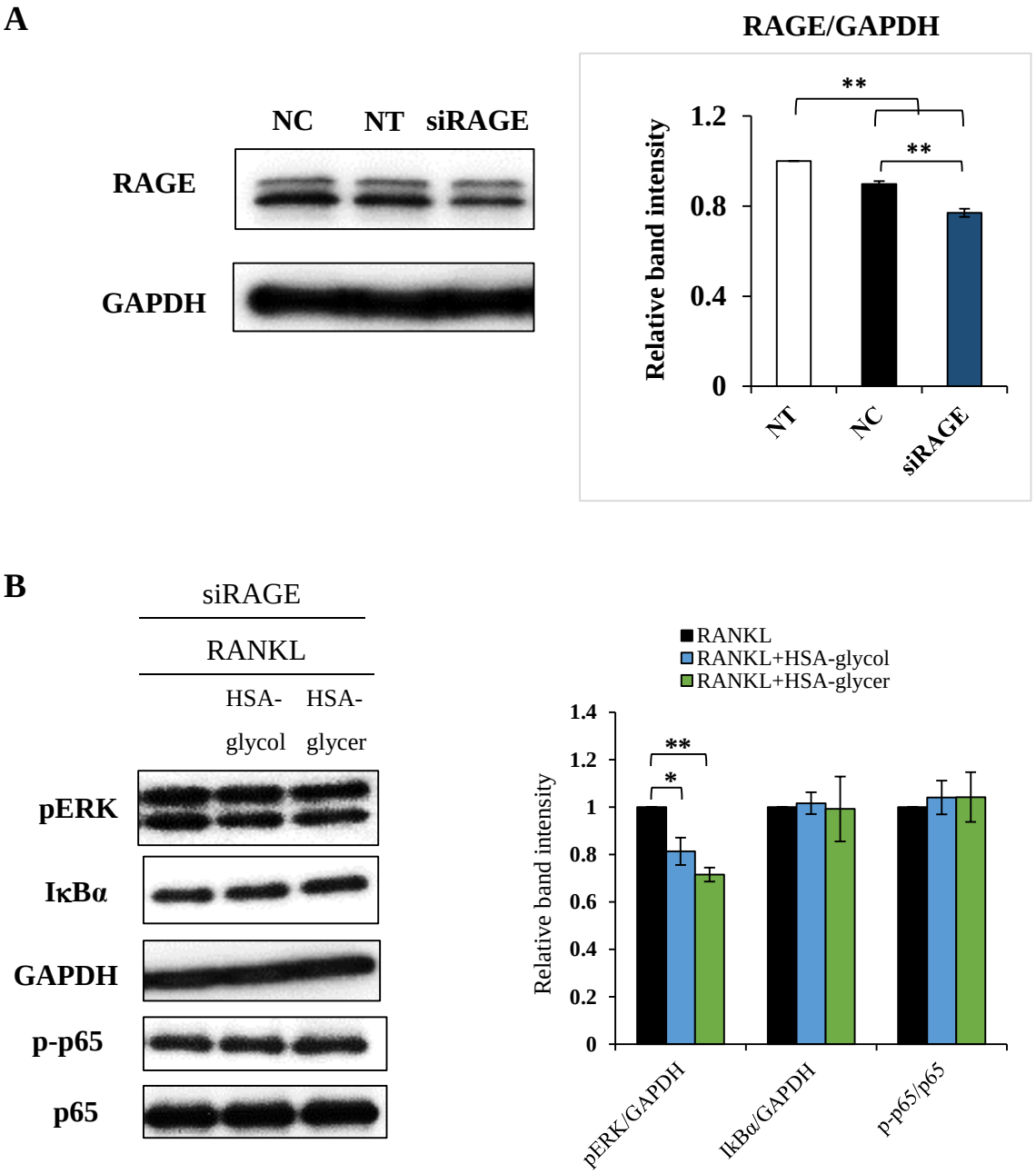

Figure 3.7: Effect of glycated-HSA on SiRAGE treated RAW264.7 cell pathway activation. A. RAW264.7 cells were transfected-using siRAGE to downregulate RAGE expression. Protein expression was analyzed by western blot and band intensity was measured using ImageJ. B. RAW264.7 cells were transfected with siRAGE and the transfected cells were then treated with RANKL with or without glycated-HSA for 30 min and then cell lysates were used to detect pathway related protein (pERK, IκBα, p-p65, p65, GAPDH) expression by western blot. Values are means ± SEM (n=3, each group), Tukey-Kramer test. **p<0.01,

*p<0.05. NT, No Transfection; NC, Negative Control; si, small interfering RAGE.

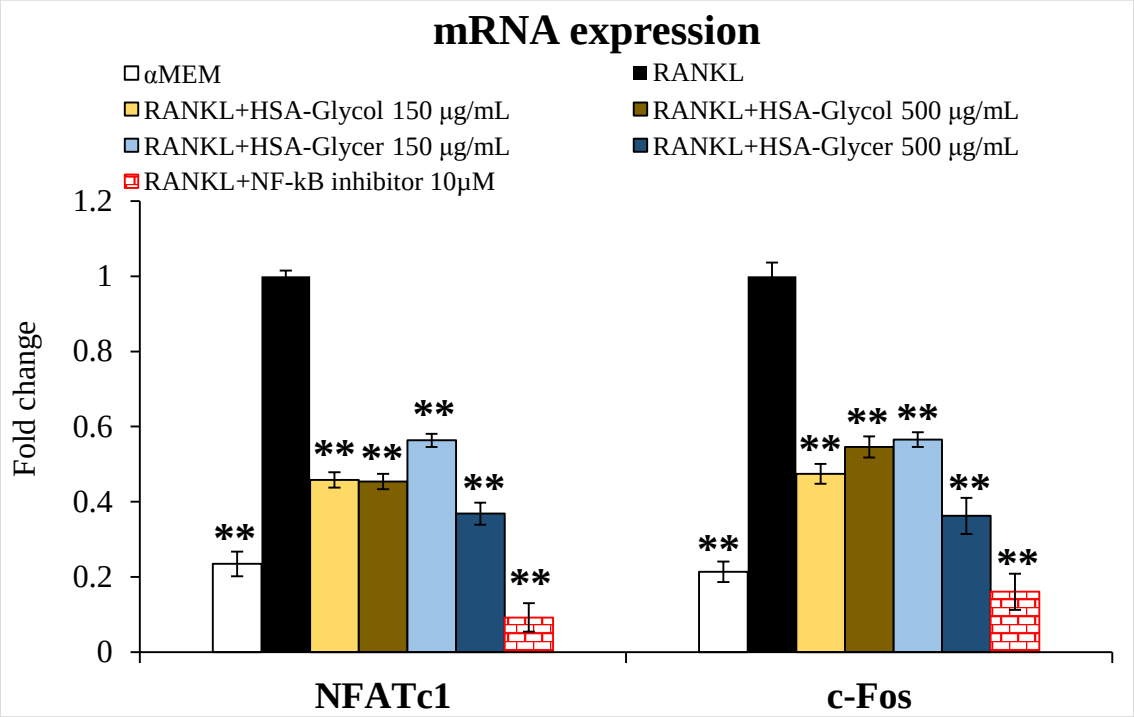

Figure 3.8: Effect of glycated-HSA on osteoclastogenic NFATc1, c-Fos mRNA expression. A. RAW264.7 cells were treated with glycated-HSA or NFκB inhibitor in the presence of RANKL for 6 h and the mRNA expression of NFATc1 and c-Fos were checked by RT-PCR. Values are means ± SEM (n=3, each group in two independent experiments), Tukey-Kramer test. **p<0.01, *p<0.05.

A

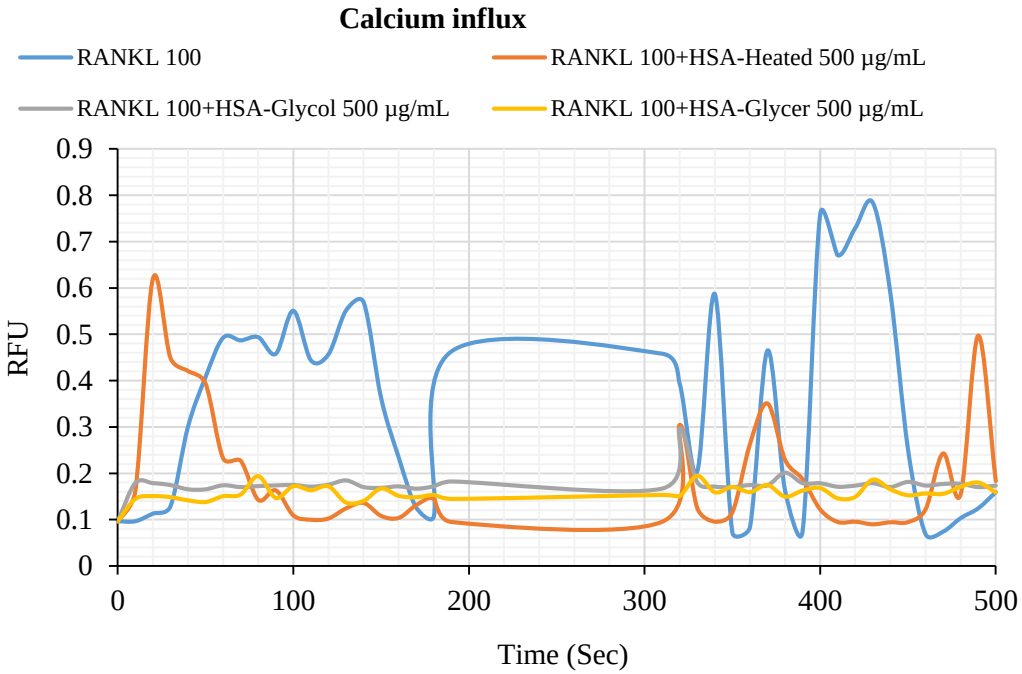

B

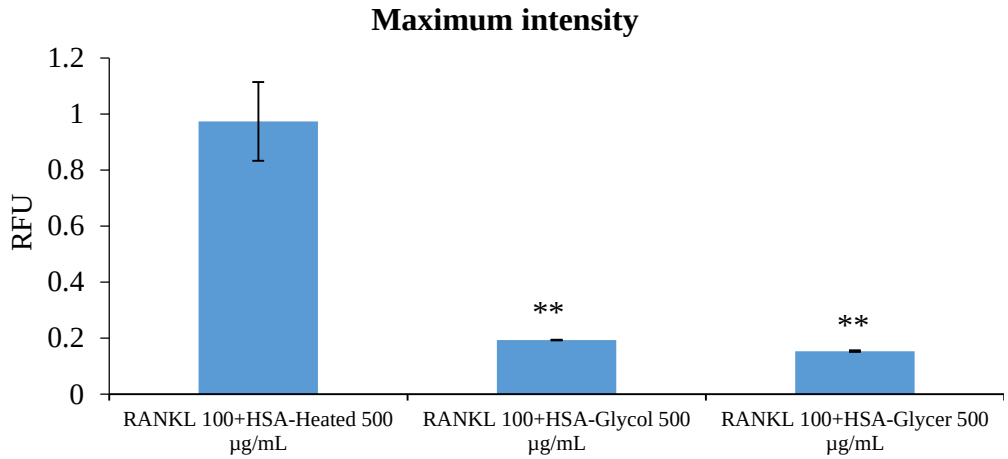

Figure 3.9: Glycated-HSA inhibited calcium influx activation. A. RAW264.7 cells were treated with glycated-HSA in the presence of RANKL. Calcium influx was checked using Fluo-8 assay kit for up to 500 seconds. B. Maximum intensity. Values are means ± SEM (n=5, each group), Tukey-Kramer test. **p<0.01, *p<0.05.

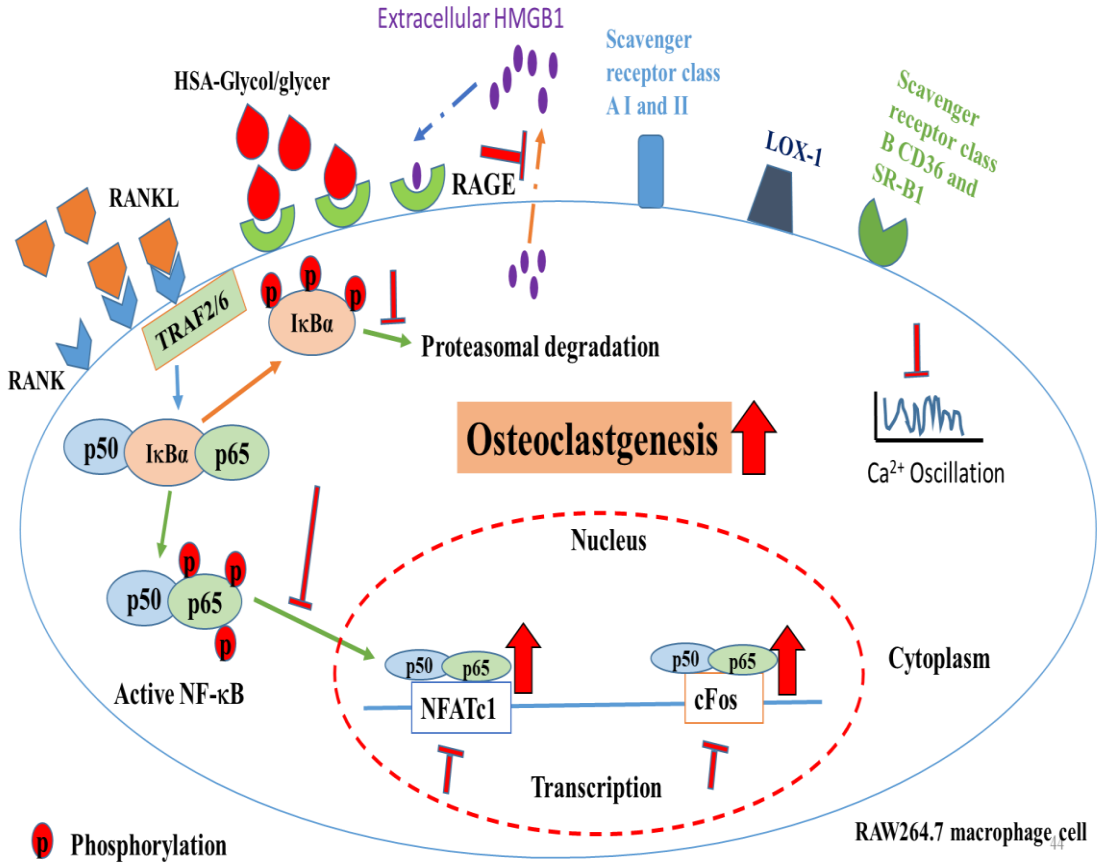

Figure 3.10: Schematic representation of mechanism of inhibition of RANKL signaling by HSA-AGEs: HSA-AGEs suppressed RANKL-induced activation of calcium influx, NFκB, c-Fos, NFATc1 and the secretion of HMGB1.

References

1 Miyamoto T (2012) Regulation of Osteoclast Differentiation and Bone Homeostasis. *Anti-Aging Med.* **9**, 161–164.

2 Soysa NS, Alles N, Aoki K & Ohya K (2012) Osteoclast formation and differentiation: an overview. *J. Med. Dent. Sci.* **59**, 65–74.

3 Hadjidakis DJ & Androulakis II (2006) Bone Remodeling. *Ann. N. Y. Acad. Sci.* **1092**, 385–396.

4 Mamun-Or-Rashid ANM, Takabe W, Yagi M & Yonei Y (2017) RANKL regulates RAW264.7 cell osteoclastogenesis in a manner independent of M-CSF, dependent on FBS, media content and cell density. *Glycative Stress Res.* **4**, 040–052.

5 Glantschnig H, Fisher JE, Wesolowski G, Rodan GA & Reszka AA (2003) M-CSF, TNFα and RANK ligand promote osteoclast survival by signaling through mTOR/S6 kinase. *Cell Death Differ.* **10**, 1165–1177.

6 Boyce BF, Rosenberg E, de Papp AE & Duong LT (2012) The osteoclast, bone remodelling and treatment of metabolic bone disease. *Eur. J. Clin. Invest.* **42**, 1332–1341.

7 Steeve KT, Marc P, Sandrine T, Dominique H & Yannick F (2004) IL-6, RANKL, TNF-alpha/IL-1: interrelations in bone resorption pathophysiology. *Cytokine Growth Factor Rev.* **15**, 49–60.

8 Jason M. H, Fiona M. C, Nathan J. P, Mark A. K & Geoffrey C. N (2011) M-CSF Potently Augments RANKL-Induced Resorption Activation in Mature Human Osteoclasts. *PLoS One* **6**, e21462.

9 Yagi M & Yonei Y (2017) Glycative stress and anti-aging: 3. The evaluation of glycative Stress: Measurement of advanced glycation end products (AGEs). *Glycative Stress Res.* **4**, 53–57.

10 Nagai R, Ikeda K, Higashi T, Sano H, Jinnouchi Y, Araki T & Horiuchi S (1997) Hydroxyl Radical Mediates Nϵ-(Carboxymethyl)lysine Formation from Amadori Product. *Biochem. Biophys. Res. Commun.* **234**, 167–172.

11 Sell DR & Monnier VM (1969) Structure E~ucidation of a Senescence Cross-link from Human Extracellular Matrix. *J. Biol. Chem.* **264**, 21597–21602.

12 Barzilay JI, Bůžková P, Zieman SJ, Kizer JR, Djoussé L, Ix JH, Tracy RP, Siscovick DS, Cauley JA, Mukamal KJ & Barzilay J (2014) Circulating levels of carboxy-methyl-lysine (CML) are associated with hip fracture risk: the cardiovascular health study HHS Public Access. *J Bone Min. Res.* **29**, 1061–1066.

13 Hein G, Weiss C, Lehmann G, Niwa T, Stein G & Franke S (2006) Advanced glycation end product modification of bone proteins and bone remodelling:

hypothesis and preliminary immunohistochemical findings. *Ann. Rheum. Dis.* **65**, 101–4.

14 Hein G, Wiegand R, Lehmann G, Stein G & Franke S (2003) Advanced glycation end-products pentosidine and N -carboxymethyllysine are elevated in serum of patients with osteoporosis. *Rheumatology* **42**, 1242–1246.

15 Saito M & Marumo K (2015) New treatment strategy against osteoporosis: Advanced glycation end products as a factor for poor bone quality. *Glycative Stress Res.* **2**, 1–14.

16 Yang D-H, Chiang T-I, Chang I-C, Lin F-H, Wei C-C & Cheng Y-W (2014) Increased Levels of Circulating Advanced Glycation End-Products in Menopausal Women with Osteoporosis. *Int. J. Med. Sci.* **11**, 453–460.

17 Zhou Z, Han J-Y, Xi C-X, Xie J-X, Feng X, Wang C-Y, Mei L & Xiong W-C (2008) HMGB1 Regulates RANKL-Induced Osteoclastogenesis in a Manner Dependent on RAGE. *J. Bone Miner. Res.* **23**, 1084–1096.

18 Lam J, Takeshita S, Barker JE, Kanagawa O, Ross FP & Teitelbaum SL (2000) TNF-α induces osteoclastogenesis by direct stimulation of macrophages exposed to permissive levels of RANK ligand. *J. Clin. Invest.* **106**, 1481–1488.

19 Sato K, Yagi M, Umehara H & Yonei Y (2014) Establishment of a model for evaluating tumor necrosis factor-α production by cultured RAW264.7 in response to glycation stress. *Glycative Stress Res.* **1**, 1–7.

20 Lee SE, Chung WJ, Kwak HB, Chung C-H, Kwack K, Lee ZH & Kim H-H (2001) Tumor necrosis factor-alpha supports the survival of osteoclasts through the activation of Akt and ERK. *J. Biol. Chem.* **276**, 49343–9.

21 Xue J, Rai V, Singer D, Chabierski S, Xie J, Reverdatto S, Burz DS, Schmidt AM, Hoffmann R & Shekhtman A (2011) Advanced Glycation End Product Recognition by the Receptor for AGEs. *Structure* **19**, 722–732.

22 Boyce BF, Xiu Y, Li J, Xing L & Yao Z (2015) NF-κB-mediated regulation of osteoclastogenesis. *Endocrinol. Metab. (Seoul, Korea)* **30**, 35–44.

23 Yamashita T, Yao Z, Li F, Zhang Q, Badell IR, Schwarz EM, Takeshita S, Wagner EF, Noda M, Matsuo K, Xing L & Boyce BF (2007) NF-κB p50 and p52 regulate receptor activator of NF-κB ligand (RANKL) and tumor necrosis factor-induced osteoclast precursor differentiation by activating c-Fos and NFATc1. .

24 Wong BR, Besser D, Kim N, Arron JR, Vologodskaia M, Hanafusa H & Choi Y (1999) TRANCE, a TNF family member, activates Akt/PKB through a signaling complex involving TRAF6 and c-Src. *Mol. Cell* **4**, 1041–9.

25 Sato K, Yagi M, Takabe W & Yonei Y (2015) Inhibitory effect of plant extract on

tumor necrosis factor-α formation from carboxymethyllysine stimulated macrophages. *Glycative Stress Res.* **2**, 191–196.

26 Mamun-Or-Rashid ANM, Takabe W, Yagi M & Yonei Y (2017) Glycated-HSA inhibits osteoclastogenesis in RAW264.7 cells depending on the glycating agents via downregulating RANKL-signaling. *Glycative Stress Res.* **5**, 00–00.

27 Hori M, Yagi M, Nomoto K, Ichijo R, Shimode A, Kitano T & Yonei Y (2012) Experimental models for advanced glycation end product formation using albumin, collagen, elastin, keratin and proteoglycan. *Anti-Aging Med.* **9**, 125–134.

28 Mamun-Or-Rashid ANM, Takabe W, Yagi M & Yonei Y (2017) Glycated-proteins modulate RANKL-induced osteoclastogenesis in RAW264.7 cells. *Glycative Stress Res.* **5**, 00–00.

29 Nomoto K, Yagi M, Hamada U, Naito J & Yonei Y (2013) Identification of advanced glycation endproducts derived fluorescence spectrum in vitro and human skin. *Anti-Aging Med.* **10**, 92–100.

30 Mamun-Or-Rashid ANM, Takabe W & Yonei Y (2016) Melatonin has no direct effect on inflammatory gene expression in CML-HSA stimulated RAW264.7 cells. *Glycative Stress Res.* **3**, 141–151.

31 Ghayor C, Correro RM, Lange K, Karfeld-Sulzer LS, Grä Tz KW & Weber FE (2011) Inhibition of osteoclast differentiation and bone resorption by N-Methylpyrrolidone. *J. Biol. Chem.* **286**, 24458–24466.

32 Arriero M del M, Ramis JM, Perelló J & Monjo M (2012) Inositol hexakisphosphate inhibits osteoclastogenesis on RAW 264.7 cells and human primary osteoclasts. *PLoS One* **7**, e43187.

33 Park KH, Park B, Yoon DS, Kwon S-H, Shin DM, Lee JW, Lee HG, Shim J-H, Park JH & Lee JM (2013) Zinc inhibits osteoclast differentiation by suppression of Ca 2+ -Calcineurin-NFATc1 signaling pathway. .

34 Yoshida H, Hayashi S-I, Kunisada T, Ogawa M, Nishikawa S, Okamura H, Sudo T, Shultz LD & Nishikawa S-I (1990) The murine mutation osteopetrosis is in the coding region of the macrophage colony stimulating factor gene. *Nature* **345**, 442–444.

35 Wiktor-Jedrzejczak W, Bartocci A, Ferrante AW, Ahmed-Ansari A, Sell KW, Pollard JW & Stanley ER (1990) Total absence of colony-stimulating factor 1 in the macrophage-deficient osteopetrotic (op/op) mouse. *Proc. Natl. Acad. Sci. U. S. A.* **87**, 4828–32.

36 Tanaka S, Takahashi N, Udagawa N, Tamura T, Akatsu T, Stanley ER, Kurokawa T & Suda T (1993) Macrophage Colony-stimulating Factor Is Indispensable for both

Proliferation and Differentiation of Osteoclast Progenitors. *Clin. Invest* **91**, 257–263.

37 Wang Y, Wang B, Fu L, A L & Zhou Y (2014) Effect of Fetal Bovine Serum on Osteoclast Formation in vitro. *J. Hard Tissue Biol.* **23**, 303–308.

38 Gstraunthaler G, Lindl T & van der Valk J (2013) A plea to reduce or replace fetal bovine serum in cell culture media. *Cytotechnology* **65**, 791–793.

39 Gu DR, Hwang J-K, Erkhembaatar M, Kwon K-B, Kim MS, Lee Y-R & Lee SH (2013) Inhibitory effect of Chrysanthemum zawadskii Herbich var. latilobum kitamura extract on RANKL-induced osteoclast differentiation. *Evid. Based. Complement. Alternat. Med.* **2013**, 509482.

40 Song I, Kim JH, Kim K, Jin HM, Youn BU & Kim N (2009) Regulatory mechanism of NFATc1 in RANKL-induced osteoclast activation. *FEBS Lett.* **583**, 2435–2440.

41 Pombinho AR, Laizé V, Molha DM, Marques SMP & Cancela ML (2004) Development of two bone-derived cell lines from the marine teleost Sparus aurata ; evidence for extracellular matrix mineralization and cell-type-specific expression of matrix Gla protein and osteocalcin. *Cell Tissue Res.* **315**, 393–406.

42 Fuller K, Owens JM, Jagger CJ, Wilson A, Moss R & Chambers TJ (1993) Macrophage Colony-stimulating Factor Stimulates Survival and Chemotactic Behavior in Isolated Osteoclasts. *J. Exp. Med.* **178**, 1733–1744.

43 Reszka AA, Halasy-Nagy JM, Masarachia PJ & Rodan GA (1999) Bisphosphonates act directly on the osteoclast to induce caspase cleavage of mst1 kinase during apoptosis. A link between inhibition of the mevalonate pathway and regulation of an apoptosis-promoting kinase. *J. Biol. Chem.* **274**, 34967–73.

44 Nakamura I, Lipfert L, Rodan GA & Duong LT (2001) Convergence of αvβ3Integrin–And Macrophage Colony Stimulating Factor–Mediated Signals on Phospholipase Cγ in Prefusion Osteoclasts. *J. Cell Biol.* **152**, 361–373.

45 Datta SR, Brunet A & Greenberg ME (1999) Cellular survival: a play in three Akts. *Genes Dev.* **13**, 2905–27.

46 Kelley TW, Graham MM, Doseff AI, Pomerantz RW, Lau SM, Ostrowsk MC, Franke TF & Marsh CB (1999) Macrophage colony-stimulating factor promotes cell survival through Akt/protein kinase B. *J. Biol. Chem.* **274**, 26393–8.

47 Barkett M & Gilmore TD (1999) Control of apoptosis by Rel/NF-κB transcription factors. *Oncogene* **18**, 6910–6924.

48 Xing L, Venegas AM, Chen A, Garrett-Beal L, Boyce BF, Varmus HE & Schwartzberg PL (2001) Genetic evidence for a role for Src family kinases in TNF family receptor signaling and cell survival. *Genes Dev.* **15**, 241–53.

49 Valcourt U, Merle B, Gineyts E, Viguet-Carrin S, Delmas PD & Garnero P (2007) Non-enzymatic glycation of bone collagen modifies osteoclastic activity and differentiation. *J. Biol. Chem.* **282**, 5691–703.

50 Takeuchi M, Takino J & Yamagishi S (2010) Involvement of the toxic AGEs (TAGE)-RAGE system in the pathogenesis of diabetic vascular complications: a novel therapeutic strategy. *Curr. Drug Targets* **11**, 1468–82.

51 Chiu Y-H & Ritchlin CT (2016) DC-STAMP: A Key Regulator in Osteoclast Differentiation. *J. Cell. Physiol.* **231**, 2402–7.

52 Park S-H, Kim J-Y, Cheon Y-H, Baek JM, Ahn S-J, Yoon K-H, Lee MS & Oh J (2016) Protocatechuic acid attenuates osteoclastogenesis by downregulating JNK/c-Fos/NFATc1 signaling and prevents inflammatory bone loss in mice. *Phyther. Res.* **30**, 604–612.

53 Abu-Amer Y (2013) NF-κB signaling and bone resorption. *Osteoporos. Int.* **24**, 2377–86.

54 Rucci N (2008) Molecular biology of bone remodelling. *Clin. Cases Miner. Bone Metab.* **5**, 49–56.

55 Sanguineti R, Puddu A, Mach F, Montecucco F, Viviani GL & Viviani GL (2014) Advanced glycation end products play adverse proinflammatory activities in osteoporosis. *Mediators Inflamm.* **2014**, 975872.